Graduate Theses and Dissertations   Graduate School

2011

A Novel Device for Cell-Cell Electrofusion

Justin T. Stewart
University of South Florida, justin.stewart75@gmail.com

A Novel Device for Cell-Cell Electrofusion

by

Justin T. Stewart

A thesis submitted in partial fulfillment
of the requirements for the degree of
Master of Science in Biomedical Engineering
Department of Chemical & Biomedical Engineering
College of Engineering
University of South Florida

Co-Major Professor: Mark J. Jaroszeski, Ph.D.
Co-Major Professor: Don F. Cameron, Ph.D.
Nathan D. Gallant, Ph.D.
Richard J. Connolly, Ph.D.

Date of Approval:
March 21, 2011

Keywords: Allograft, Electropermeabilization, Fusogenic, Immunosuppression,
Xenograft

Dedication

I must first dedicate this work and give thanks to God; with Him all things are possible. I would also like to dedicate this work to my supportive and loving wife, Dulche. Thank you for being patient with me the many nights I was in the library and the lab trying to accomplish my goals. I also thank you for your continuous support; I would not have accomplished this without you. I must also dedicate this body of work to the best children a father could ask for (Elijah and Akayla). There were many nights I could not spend vital family time. Without your continuous support and numerous sacrifices, I would not have been able to focus my attention on my endeavors. I want you both to know that you have exceeded my expectations in life and you keep your father's heart blissful. Lastly, this is dedicated to my parents. A mother's love is like no other and it kept me sane the many times I considered what major I was pursuing. I also thank you for your endearing and boundless love. Thank you for understanding when I could not call because I was conducting an experiment or studying for an exam. In addition, I would also like to thank my Dad; the man that showed me how to be a real man through his actions. There are many times I wonder where I would be if I had not been blessed with your love. Your many prayers have been answered and I thank you for sharing valuable ideas and thoughts with me. I am still working on patterning my life after the poem "If". Thanks you for standing by me from the time at NCSU all the way to now. I pray I can be half the father to Elijah that you have been to me.

Acknowledgements

I would like to begin my acknowledgements by thanking my Graduate Committee Co-Major Professors Dr. Mark Jaroszeski and Dr. Don Cameron for their guidance and for allowing me an opportunity to conduct research in their laboratories. In conjunction, I would also like to thank my Committee Members Dr. Nathan Gallant for lending his expertise and Dr. Richard Connolly for his efforts in my biological training and for assisting me with ideas of how to methodically conduct this research study.

I am grateful to all three of my mentors: Dr. Sylvia Thomas, Electrical Engineering Professor, Dr. John Wolan, Chemical Engineering Professor and Mr. Bernard Batson, Director of Diversity and Outreach Programs. Their patience, willingness to help and candid advice assisted me in a difficult, yet necessary transition in life. I am thankful for the opportunity to call you mentor and I pray I can one day return the favor. Support for this work was provided by NSF S-STEM award DUE# 0807023.

I would also like to thank those who were responsible for assisting me with the logistical challenges of this research study: Dr. Charles Szekeres, Mr. Charles Manning, Ms. Julie Kahn, Mr. Jose Rey, and Mrs. Taryn Chapman. Last, but most certainly not least, I would like to sincerely thank my friend, Ms. Alexandra Oliveros, Electrical Engineering Doctoral Candidate and Atomic Force Microscope (AFM) Manager in the Silicon Carbide Lab, for her continuous positive presence and quality AFM work contributed to this research study.

Table of Contents

ii

List of Tables

List of Figures

vi

List of Equations

List of Abbreviations

AC (Alternating Current)

AT (Adenine Thymine)

ATCC (American Type Culture Collection)

B16-F10 (Murine Melanoma Cells)

C (Centigrade)

CAD (Computer-Aided Design)

cm^2 (Centimeters Squared)

CMFDA (5-chloromethylfluorescein diacetate)

CMTMR (5-(and-6)-(((4-chloromethyl)-benzoyl)amino)tetramethyl-rhodamine)

CO_2 (Carbon Dioxide)

DAPI (4', 6-diamidino-2-phenylindole)

DC (Direct Current)

DMEM (Dulbecco's Minimum Essential Medium)

DNA (Deoxyribonucleic Acid)

DPBS (Dulbecco's Phosphate Buffered Saline)

EDDS (Ethylenediamine-*N*,*N*′-disuccinic Acid)

EDTA (Ethylenediaminetetraacetic Acid)

EMT (Emergency Medical Technician)

et al (Latin abbreviation for 'and others')

F (Fahrenheit)

FACS (Fluorescence Activated Cell Sorting)

H4 (Human Neuroglioma Cells)

HaCaT (Human Adult Low Calcium High Temperature Cell)

HSC (Human Sertoli Cell)

ITS (Insulin, Transferrin, and Selenium)

µl (Microliter)

ml (Milliliter)

mM (Millimolar)

nm (Nanomolar)

NREC (Nanotechnology Resource and Education Center)

PEG (Polyethylene Glycol)

PISH (Pig Islet Sertoli Hybrid)

RFC (Relative Centrifugal Force)

RSC (Rat Sertoli Cell)

SiC (Silicon Carbide)

USF (University of South Florida)

w/v (Weight per unit volume)

Abstract

Cell transplantation therapy is a potentially powerful tool and can be used to replace defective cells with healthy cells. This offers the possibility of alleviating the destructive symptoms for many diseases such as Parkinson's disease, Alzheimer's disease, stroke, spinal cord trauma, Type I diabetes and many more. While there are many diseases that could be positively impacted from cell transplantation therapy, the focus of this research is insulin dependent, Type I Diabetes.

The Islets of Langerhans are composed of various types of cells located in the pancreas and are responsible for a variety of biochemical functions. Specifically, the beta Islet cells are responsible for production of the hormone insulin that regulates and aids in biosynthesis of glucose. Transplantation of isolated allografted pancreatic islets, which contain insulin producing cells, into diabetic rats has proven to be highly successful. However, these transplantations involve using medications for long term immunosuppression to defend against an undesired host immune response. Immunosuppressive medications are both costly and illicit additional side effects that can be detrimental to the host. This research focuses on the use of testicular derived Sertoli cells that have been publicized to provide localized immunoprotection.

Electrofusion is a process that can be used to fuse homogeneous and heterogeneous cell types by promoting the creation of micropores in the cell's lipid bilayer. This renders the cell temporarily fusogenic, or capable of facilitating fusion.

x

Cells must then be brought into contact with one another via mechanical, chemical or viral means. This research study proposes to optimize electrofusion technology to create novel, secretory hybrids composed of Islet and Sertoli cells that are immunoprotected and produce insulin in response to a glucose challenge.

The components of the electrofusion device include a Sterlitech 0.2 μm microporous membrane, a woven cellulose absorbent pad, two aluminum electrodes and a chamber body and top injection molded using Delrin. Preliminary experiments using B16-F10 murine melanoma cells incorporated with centrifugation to increase cell to cell contact resulted in an average fusion yield of 18.9% ± 8.1 SD using a field strength of 2500 V/cm, 8 pulses and a 250 μs pulse length. Additionally, lab synthesized electroporation buffers containing 8.5% sucrose (w/v) and 0.3% glucose increased total and viable fusion yields to 37.1% ± 9.3 SD and 13.8% ± 2.1 SD, respectively. These results showed promise and should be further validated with additional cell lines and tissues to corroborate reproducibility.

Chapter 1. Introduction

1.1 Overview of Electroporation and Electrofusion

Electrofusion is a process that can be used to fuse homogeneous and heterogeneous cell types by a phenomenon known as electropermeabilization. This phenomenon occurs due to a temporary breakdown of the cell's lipid bilayer in the cell membrane as a result of increased transmembrane potential. The first cell fusion publication of this observation was in 1979 (Senda et. al). The permeabilization of the cell membrane is also believed to create aqueous filled micropores in the bilayer (Teissie et al, 1999; Zimmerman et al, 1976). An additional study using Direct Molecular Dynamics Simulation suggests that the initial pore formation is a result of water defects in the interior of the membrane as opposed to the lipid headgroups in the lipid bilayer (Tieleman, 2004). It has been shown that cells in an electroporated state can fuse to form hybrids.

Cell fusion technology has utility because it can be used to create several types of biological hybrids that can impact biomedicine. This most common application of cell fusion is for the creation of antibodies in vitro. Antigent presenting cells from the body, such as dendritic cells, are harvested and fused with primary cancerous tumor cells. These cells are then infused back into the person to formulate tumor antigens to the host and subsequently train the immune system to destroy the cancer cells that comprise the

1

tumor. This has been accomplished in clinical trials and has shown success in tumor regression of human renal cell carcinoma (Kugler et al, 2000). Another common biomedical application of cell fusion includes the hybridization of B cell and myeloma cells are that are grown in culture to produce antibodies (Panova at al, 1995). They are then harvested and used as reagents. Another biomedical use of electrofusion included engineering infracted rat heart tissue to successfully improve systolic and diastolic functionality (Zimmermann et al, 2006). Cell electrofusion technology has recently been employed to characterize a novel glucose-responsive insulin-secreting cell line, BRIN-BD11 (McClenaghan et al, 2011). It is envisioned that sertoli cells can be fused to any cell type to provide localized immunoprotection upon transplantation (Sandberg et al, 1996; Sandberg et al, 1997; Selawry et al, 1993). One example of this type of use is the fusion of sertoli cells with islet cells. This type of construct could provide immunoprotection to transplanted islets so that they are not rejected by the host.

For all types of cell-cell fusion, it is necessary for the cells to be in a fusogenic (electroporated) state and in contact with each other in order for fusion to occur. The need for cell contact has been the most problematic and limiting aspect of fusion technology. Some of the methods that have been used to achieve contact are electrical, mechanical, chemical and viral means.

 Dielectrophoresis is an electrically based method used to align cells prior to electroporation by passing an alternating current (AC) through a cell suspension (Zimmerman, 1982). The alignment that occurs from the AC field in dielectrophoresis increases cell to cell contact which in practice can increase electrofusion yields when used in conjunction with direct current (DC) fields. Dielectrophoresis is a common

2

method for achieving cell to cell contact. However, this method is counterproductive due to thermal interactions, otherwise known as joule heating, that decrease viability and cell function arising from the alternating current. This method may not be practical when used in conjunction with cell transplantation due to the diminishment of cell functionality. In addition, electrophoresis involves the use of expensive generators that may not be commonly used in most research laboratories.

Cell to cell contact can also be induced using chemical or viral means. Polyethylene glycol (PEG) is a low toxicity, polyether compound that can be used to induce fusion (Davidson et al, 1976). PEG has also been used to disrupt the membranes of difficult to transfect cell lines and to form heterokaryons where cytoplasms and membranes of cells have merged (Dragic et al, 1992). Additionally, a study was accomplished that showed using PEG fused cells were equally as immunogenic as electrically fused cells (Lindner et al, 2002). However, even though PEG is a low toxicity compound, the introduction of external chemicals to cells for transplantation may cause irreparable damage to the host and may also affect viability of the transplanted cells. Hybridoma technology, initially discovered by Georges Köhler and Cesar Milstein in 1975, forms antibodies using PEG or Sendai virus fused B-cells with immortalized myeloma cells that are monoclonal, or operate with a single specificity (Pandey 2010).

Mechanically facilitated cell-cell electrofusion involves using mechanical forces to bring cells into contact with each other (Jaroszeski et. al, 1994). This can include placing cells between adherent surfaces and forcing them together. Depending on the mechanical means, this can be very useful in creating and quantifying cell hybrids using flow cytometry (Jaroszeski et al, 1994). However, this type of cell to cell contact can be

3

cumbersome depending on the method utilized. Electrofusion devices can be difficult to manipulate and may involve several steps prior to and between uses. This may introduce a dilemma when time is a factor for cell viability, especially when multiple samples need to be fused as is often the case.

Centrifugation is another mechanical method that has been used to increase cell to cell contact (Teissie and Rols, 1986). This method incorporates the use of centrifugal forces and can be used for homogeneous and heterogeneous cell types. While this method may increase contact, viability may also decrease due to high centrifugal forces. Centrifugation parameters need to be optimized and would be unique for each cell type.

1.2 Electrofusion Devices at the University of South Florida

The University of South Florida began researching electrofusion methods in the early 1990's. Fabricated electrofusion chambers were created in the lab in an effort to accomplish fusion by means other than chemical, viral or centrifugal methods. The initial chamber used vacuum to draw layers of cells onto two microporous membranes. The two membranes were then forced together by mechanical means and fused using direct current (DC) pulses. Fusion was accomplished but problems persisted with low yields, poorer fusion viability and a cumbersome chamber design. The second generation chamber used a vacuum to deposit cells onto a single membrane. This was a simplified chamber, but suffered from poor contact between cells on the membrane which lead to low fusion yields. The third generation electrofusion device replaced the vacuum system and works through absorption of a cell suspension through a porous membrane onto an absorbent pad. The device is also for single use and can be scaled in size in accordance with the need of the research. The optimizations, as well as the potential advantages, are discussed as part of this thesis.

Chapter 2. Research Goals

There are several significant biomedical applications for fused cells in use today such as antibody production and cancer treatment. There are additional potential uses for fusion products in cell transplantation that can be envisioned. These facts coupled with the difficult nature of achieving cell contact during fusion clearly indicate the need for an efficient and easy to use fusion method.

The third generation USF fusion chamber could easily provide a solution. It is small, easy to mass produce, sterilizable, scalable, easy to use, and only requires a DC generator to induce fusion. This chamber has been designed, but it is still untested and uncharacterized. Therefore, the overall goal of this study is to characterize and optimize this chamber. This will be done by accomplishing a set of smaller goals which were to:

1. Develop Cell Fusion Detection and Quantitation Methods. This was a necessary step as a means for discriminating fused cells from unfused cells was necessary of investigating the chamber.

2. Characterize Membrane and Absorbent Pad. Since the chamber had never been used to deposit cells, it was necessary to determine select a membrane that had the best potential of working well.

6

3. Implement a Basic Cell Fusion Protocol. A basic protocol for introducing cells into the chamber, performing fusion, removing and removing the cells had to be developed and tested. Murine B16 cells were used as a model cell line.

4. Fuse a Variety of Cell Lines. Keratinocyte, neuroglioma, and sertoli cell lines were fused using the chamber to support that the chamber has utility of a number of cell lines.

5. Investigate Potential Improvements. The use of centrifugation and novel solutions for fusion were identified and experimentally tested potential ways to improve fusion chamber and its use.

Chapter 3. Materials and Methods

3.1 Cell Lines and Culture Methods

3.1.1 B16-F10 Murine Melanoma Cells

The primary cell line that was used both initially and consistently used throughout the study was murine B16-F10 (ATCC-6475; American Type Culture Collection, Manassas, VA) melanoma cells. These cells have been and are currently used in the Drug & Gene Delivery Lab for a multitude of studies including electroporation, electrophoresis, electrofusion and drug delivery. The B16-F10 murine melanoma cell line was cultured in McCoy's 5A Medium (Iwakata & Grace Modified with L-Glutamine; Mediatech, Inc., Manassas, VA) and was supplemented with 10% weight per volume (w/v) heat inactivated fetal bovine serum (FBS; Fisher Scientific, Pittsburg, PA) and 0.1% w/v Gentamicin Sulfate (50 mg/ml solution; Mediatech, Inc., Manassas, VA). The cells were cultured in an incubator that was maintained at 37°C and supplemented with 5% carbon dioxide (CO_2).

3.1.2 Human Keratinocyte Cells (HaCaT)

In conjunction to murine B16-F10 cells, human (HaCaT; Human Adult Low Calcium High Temperature, Dr. Sunil Chada, Introgen Therapeutics, Houston, Texas) keratinocytes were also used in this research study to optimize the electrofusion device.

8

These cells have been used in dermatology research such as a human skin modeling system for vitamin D_3 metabolism (Lehmann, 1997). The human keratinocyte cell line was cultured in Dulbecco's Modification of Eagle's Medium with 1 gram per liter (g/l) of glucose, L-glutamine and sodium pyruvate (Mediatech, Inc., Manassas, VA) and was supplemented with 10% w/v heat inactivated fetal bovine serum (Fisher Scientific, Pittsburg, PA) and 0.1% w/v gentamicin sulfate (50 mg/ml solution; Mediatech, Inc., Manassas, VA). Similarly to the murine B16-F10 cells, the HaCaT cells were cultured in an incubator that was maintained at 37°C and supplemented with 5% carbon dioxide (CO_2).

3.1.3 H4 Neuroglioma Cells

H4 Neuroglioma Cells (H4; ATCC HTB-148) were proved by Ms. Alexandra Oliveros, doctoral candidate from the University of South Florida Electrical Engineering's Silicon Carbide (SiC) Lab. The neuroglioma cell line, also referred to as H4, was cultured in Advanced Dulbecco's Modification of Eagle's Reduced Serum Medium with D-glucose, non essential amino acids, 110 mg/l sodium pyruvate (Invitrogen; California) and was supplemented with 10% w/v heat inactivated fetal bovine serum (Fisher Scientific, Pittsburg, PA), 1% w/v Penicillin-Streptomycin (Invitrogen; California) and 2 millimolar (mM) L-Glutamine (Invitrogen; California). Similarly to the murine B16-F10 cells and the HaCaT cells, the H4 cells were cultured in an incubator that was maintained at 37°C and supplemented with 5% carbon dioxide (CO_2).

3.1.4 Human Sertoli Cells

Human Sertoli Cells (HSC) were provided by Dr. Don Cameron, Pathology and Cell Biology Laboratory, USF College of Medicine. Dissimilar to the previously mentioned cell lines, the HSC were immortalized by proprietary means and characterized for proliferation (John et al, 2010). These cells were also used in this research study to optimize the electrofusion device using both homogeneous and heterogeneous cell fusion. Immortalized HSC have not been used in conjunction with electrofusion and successful research has several positive implications. The human sertoli cells were cultured in Dulbecco's Modified Eagle Medium: Nutrient Mixture F-12 (DMEM/F12; Hyclone Laboratories; Logan, Utah) supplemented with F12, 2.50 mM L-glutamine and 15 mM (4-(2-hydroxyethyl)-1-piperazineethanesulfonic acid (HEPES), which maintains a constant pH despite changes in CO_2. The medium was also supplemented with 1% Penicillin/Streptomycin (Sigma, St. Louis, MO), 5% Heat Inactivated Fetal Bovine Serum (Fisher Scientific, Pittsburg, PA) and 0.1% Gentamicin Sulfate (Cellgro, Manassas, VA).

3.2 Fluorescent Dyes and Cell Staining

This research involved the use of various types of fluorescent dyes to detect and quantitate fusion. Vybrant™ Cell-Labeling Solutions DiO and DiI (Molecular Probes, Eugene, OR) was one type. The chemical formulas were not provided from the company but they both are long chain dialkylcarbocyanines that are considered stable and bright, lipophilic fluorescent dyes. The concentrations of these dyes can be adjusted for fluorescent microscopy or flow cytometry. The dyes were shipped in a ready to use 1 ml

vials and did not need to be reconstituted. Spectral characteristics for DiO and DiI include absorptions of 484 nanometers (nm) and 549 nm and emissions of 501 nm and 565 nm, respectively. The protocol for staining with DiO and DiI included exposing cells to 4 µl/ml concentration of each dye with the cells in suspension.

In addition to using Vybrant™ Cell-Labeling Solutions DiO and DiI, Cell Tracker™ Green 5-chloromethylfluorescein diacetate (CMFDA, Invitrogen; Carlsbad, CA) and Cell Tracker™ Orange 5-(and-6)-(((4-chloromethyl)-benzoyl)amino)tetramethyl-rhodamine (CMTMR, Invitrogen, Carlsbad, CA) were also utilized for fluorescent microscopy and flow cytometry. The CMFDA and CMTMR dyes were supplied in 1 mg solid aliquots and had to be reconstituted in sterile dimethyl sulfoxide (DMSO; Sigma, St. Louis, MO). DMSO volumes of 430 µl and 360 µl were added to the CMFDA and CMTMR vials, respectively. The absorption and emission data for CMFDA is 492 nm and 517 nm and for CMTMR is 541 nm and 565 nm, respectively. Concentrations of 25 µl of CMFDA and 45 µl of CMTMR per 12 ml of media in a culture flask were sufficient in detecting fluorescence for microscopy. Control images of CMFDA and CMTMR individually stained cells, an aliquoted 1:1 ratio mix and fused cells were captured and will be displayed in the results section of this thesis. The same dyes were later used for flow cytometric analysis and fusion quantification. The optimized concentration for CMFDA was 1.5 µl/50 ml of medium and for CMTMR was 13.5 µl/50 ml of medium. As with the previous dyes, the CMFDA and CMTMR were added to fresh pre-warmed medium to preserve cell viability.

11

Dyes were added to the media in 75 square centimeter (cm^2) polystyrene cell culture flasks that the cells were grown in. Cultures with an approximate confluency of 80% of the desired cell type were used throughout this study. The dyes were added with fresh, warmed medium to preserve cell viability. The flasks were then incubated for 30-45 minutes and viewed under a fluorescent microscope to confirm the cells were stained. When flow cytometry was planned as an evaluation tool, microscopy could not be used to detect fluorescence due to the significant decrease in magnitudes of the dyes.

3.3 Stained Cell Preparation for Fusion

Post incubation, the medium was discarded and each flask was rinsed three separate times with 10 ml of Dulbecco's Phosphate Buffered Saline modified with Calcium and Magnesium (D-PBS, Hyclone Laboratories; Logan, Utah) supplemented with 0.1% w/v gentamicin sulfate (50 mg/ml solution; Mediatech, Inc., Manassas, VA). The cell monolayer was then treated with 2 ml of 0.05% trypsin (Mediatech, Inc.; Manassas, VA) and incubated between 8-15 minutes (depending on cell type) at 37°C. Trypsin is an enzyme that cleaves the peptide chains between the cells. This released the cells from the monolayer they formed at the bottom of the flask. Next, in order to stop the trypsinization process, 6 milliliters (ml) of medium supplemented with FBS was added for a final concentration of 1 ml to 3 ml (1:3, trypsin to medium). The cell detachment was verified using a microscope and a cell scraper was used to dislodge any remaining attached cells. The 8 ml contents of each flask were then transferred to either a 15 ml or 50 ml conical tube. The conical tubes were then placed in a centrifuge

(Eppendorf, Model 5810 R) for 5-7 min at 220 relative centrifugal force (RCF). These parameters were also dependent on cell type. The HSC required less centrifugal forces and thermal cycling in order to maintain viability.

Cell washing is a process in which extracellular debris and residual dye are removed with a sterile, non-binding solution. For the immortalized cell lines used in this research study, D-PBS was the solution of choice. D-PBS is a balanced salt solution that maintains a cell's physiological and structural integrity. Most importantly, the solution maintains an ideal pH balanced environment. However, as with anything else biological, this is subject to change dependent on the cell line. D-PBS could not be used for the HSC to maintain pre and post cell fusion viability. These cell lines were washed with previously used medium that was collected during harvesting and cell culturing. For each cell line, the washing process was accomplished three times per flask.

The next step in the protocol after staining and cell washing was to complete a cell count. Cell counting allows one to determine the cell density (cells/ml). Upon completion of cell washing, the supernatant was discarded and the residual solution on the walls of the container was allowed to flow to the bottom for about 1-2 minutes. The cell pellet that formed at the bottom of the container during the centrifugation process was then resuspended in the residual solution. A 10 μl aliquot of the original cell suspension was then removed and added to a pre-filled well containing 90 μl of normal saline (VEDCO®, Saint Joseph, MO). The solution was pipetted fifteen times to ensure efficient mixing and then a 20 μl sample of that solution was added to another pre-filled well with 80 μl of normal saline. The pipetting process was completing in the same

13

manner and an additional 20 µl sample was added to another pre-filled well containing 80 µl of normal saline. The final diluted suspension was then added in a 1:1 ratio of cell suspension to 0.4% Trypan Blue ($C_{34}H_{28}N_6O_{14}S_4$); ((3Z,3'Z)-3,3'-[(3,3'-dimethylbiphenyl-4,4'-diyl)di(1Z)hydrazin-2-yl-1-ylidene]bis(5-amino-4-oxo-3,4-dihydronaphthalene-2,7-disulfonic acid; Sigma, St. Louis, MO). Trypan blue is a viability stain commonly used in microscopy to determine cell viability and cell density. The solution stains non-viable cells by permeating the cell membrane and appears blue in color. The dye does not permeate viable cell membranes thereby allowing one to count viable and non-viable cells and determine a viability percentage. In this research, Trypan Blue staining was used in conjunction with a hemocytometer (Hausser Scientific; Horsham, PA). The hemocytometer contains ten distinct squares that can be viewed during microscopy to perform the manual counts of viable and non-viable cells. Cell counts were completed in triplicate and averaged to increase the accuracy of reporting. For our research purposes, experimental viabilities less than 95% were terminated. The viability was calculated with the following equation:

$$Viability_{Average} = \frac{Viable\ Cells\ Counted_{Average}}{Total\ Cells\ Counted_{Average}}$$ (Equation 1)

After the cell counts were performed on a quantity of stained and washed cells, the volume of the cell suspension was measured with a pipette and recorded for cell density

14

and total cell calculations. Total cells were calculated using the following standard

equation:

$$Total\ Cells = \frac{Avg\ Live\ Cells}{1.0\mu L} \ x\ \frac{1000\mu L}{1mL}\ x\ (Dilution\ Factor)\ x\ Total\ Volume \qquad \text{(Equation 2)}$$

Lastly, the cell density could be calculated. Examples of average cell densities, viabilities

and total cell calculations will be reported in the results section of this thesis.

$$Cell\ Density = \frac{Total\ Cells}{Total\ Volume} \qquad \text{(Equation 3)}$$

In order to mix the CMFDA and CMTMR samples in equal ratios, volume

adjustments were made depending on the average total number of viable cells counted.

Equal mixing was vital when more than one dye was used; at least if the goal was to

visualize the mixing of the two. For example, dual fluorescence, red to green fusion

emitting a yellowish-orange fluorescence, would suggest a hybrid cell construct when

using a homogeneous cell mixture. It was theorized that a one-to-one mixture of the two

different cell dyes would optimize dual fluorescence. However, this dual fluorescence

would not be the final indicator of total fusion. The next formula was used to calculate

the volume of diluent:

15

$$V_2 = \frac{C_1 V_1}{C_2} = \frac{Total\ Cells}{C_2} \qquad \text{(Equation 4)}$$

The desired concentration, seen above as C_2, were known and determined by

calculations. Once the total cells were calculated from equation two, V_2 representing the

final volume for the desired concentration was calculated. The final volume (V_2) was

then subtracted from the initial volume (V_1) to provide the amount of diluent to add to the

each stained sample. Once this step was accomplished, the samples were adjusted

according to the calculations and could be mixed in a 1:1 ratio prior to electroporation.

3.4 Standard Electrofusion Protocol

The next step in the protocol was to place a suspension containing the cells into

the electrofusion chamber and induce contact. Contact was achieved by allowing the

aqueous phase of the cell suspension to wick through the pores of a membrane into an

absorbent material. Thus, a thick cellular paste would remain on the membrane surface.

Details of the fusion chamber how contact was achieved are described in section 3.7

Electrofusion Chamber. The final step in the protocol was to electroporate the cells in the

chamber. This was accomplished using an electroporator (ECM 830, BTX-Harvard

Apparatus) that had several adjustable parameters that were dependent upon the cells

being fused. The electroporator delivered square-wave direct current pulses that can

render cells fusogenic. These electrical pulses create micropores in the cell membrane

that permit membrane fusion and cytoplasmic mixing for cells in contact with one

another. The adjustable parameters include the voltage, number of pulses, pulse length

16

and time interval between pulses. Optimized parameters for different cell lines were results of this study. Generally, the applied voltage range in this study was from 800 to 1000 volts. This translated to applying an electric field strength of 2000 to 2500 volts per centimeter to the cells. The pulse lengths ranged from 250 to 300 microseconds and the interval remained constant at 1.0 second. The temporary micropores in the cell membrane were allowed to anneal, or close, after electrical treatment. This process was facilitated by placing calcium and magnesium supplemented D-PBS into contact with the cells in the fusion chamber and then incubating at 37°C for approximately thirty minutes. The samples were then removed from the chamber and viewed by fluorescent microscopy or transferred to tubes for analysis by flow cytometry.

3.5 Electrofusion Chamber

The intended design of the electrofusion chamber was to facilitate cell to cell contact prior to electroporation. It was also designed to allow the application of high intensity electric fields to the contacted cells that would impart a fusogenic state by creating small micropores in the cell membranes. If the cells were in contact during this temporary phase of electropermeabilization, fusion of cell membranes would be probable. This was accomplished by placing an aliquot of a cell suspension of a desired concentration into the top of the chamber. The top has a rectangular shaped crevice allowing the cell suspension to pass through onto a porous membrane. Beneath the porous membrane is an absorbent pad. The porosity allows the solution from the suspension to wick through onto the absorbent pad and thereby leaving a viscous cellular paste, as shown in Figure 1.
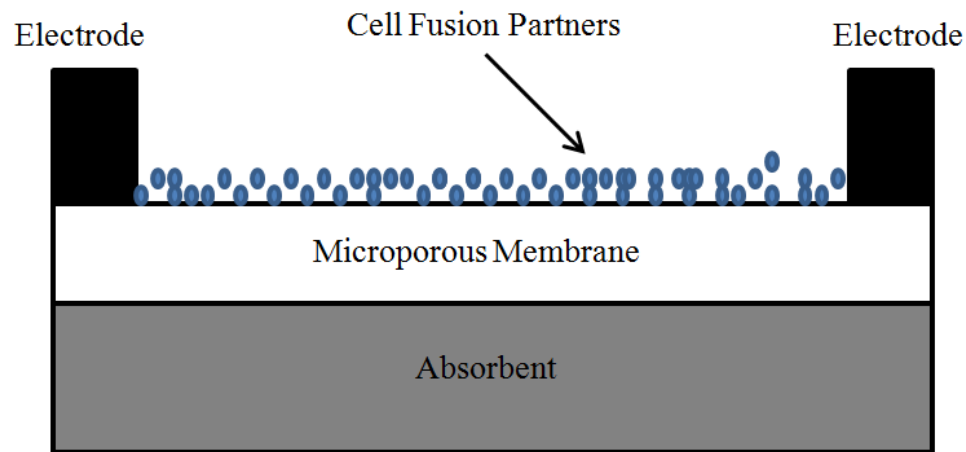
Figure 1 Schematic of Microporous Membrane and Absorbent

The absorption also facilitates cell to cell contact which is necessary for fusion. Direct current pulses were delivered through the cellular paste via aluminum electrodes that were built into the chamber. These electrodes were located on two sides of the membrane. Since the entire chamber was a closed system except for the top crevice, the cell suspension with the fused samples could be easily withdrawn using a pipette and a desired solution. The cuvette was designed to fit any commercially available cuvette holder and can be used in conjunction with any electrical generator. The chambers are depicted in Figure 2.

Figure 2. Electrofusion Chamber

3.5.1 Electrofusion Chamber Specifications

Detailed drawings and schematics of the electrofusion chamber were created using AutoCAD Software. Figure 3 shows the length and width of the top of the chamber main body, without the cap. The dimensions were approximately 0.5 inches (in) ≈ 12.7 millimeters (mm), respectively.
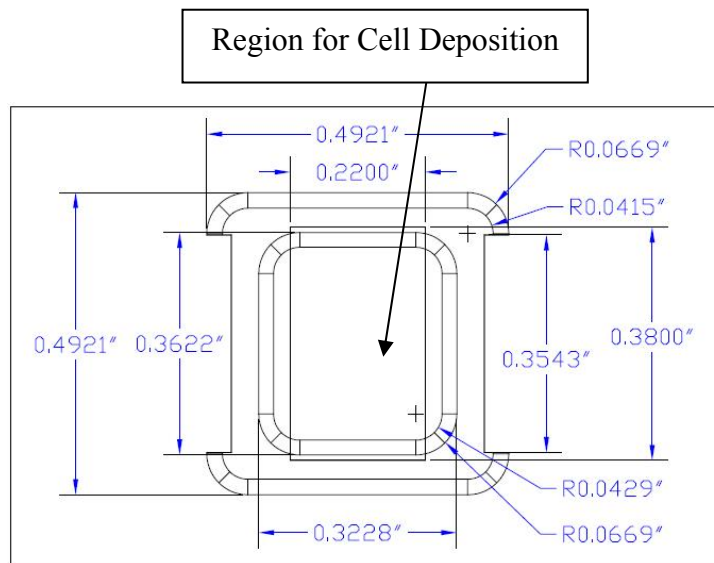
Figure 3. Dimensions of the Fusion Chamber Main Body (Top View)

However, the region for cell deposition indicated in the figure was 0.22 in (≈ 5.59 mm) in length and 0.35 in (≈ 8.89 mm) width. These dimensions were important in calculating the surface area to determine the number of cell monolayers ideal for deposition and fusion. Figure 4 shows a side view of the main chamber body. There were multiple grooves molded into the body which allowed the aluminum electrodes to rest along the sides of the body and fit properly. The body of the chamber measured 1.46 in (37.1mm) in overall length.

20
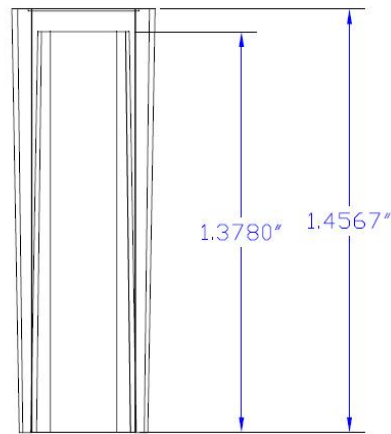
Figure 4. Main Fusion Chamber Body (Side View)

The electrodes were a vital element of the chamber. As indicated in Figure 4, body of the cuvette was slightly angled from bottom to top and contained grooves indented to hold the electrodes in place. The electrodes were made from aluminum which is a good and inexpensive conductor of current. They were designed to have a 180 degree curve on one end so that they can fit tightly against the chamber body and then make contact with the porous membrane. The dimensions as well as the shape of the electrodes are shown in Figure 5 in conjunction with an enlarged view of the 180 degree curve.
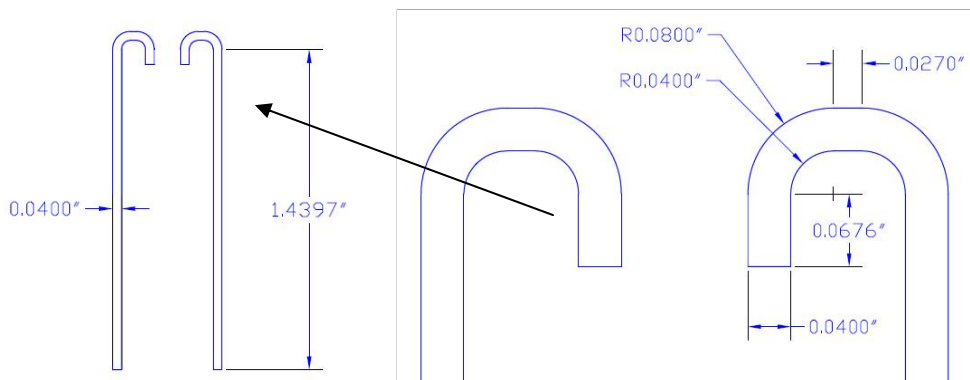
Figure 5. Electrodes

21

The three dimensional structure of the main chamber body is shown in Figure 6. The figure also indicates a recessed area to accommodate the absorbent pad and membrane. This was the surface area used for deposition cells into layers for fusion. The figure also indicates grooves to hold the electrodes in place. A three dimensional diagram of the assembled fusion chamber is shown in Figure 7. This diagram shows the relationship between the main chamber body, both electrodes, and the chamber top.
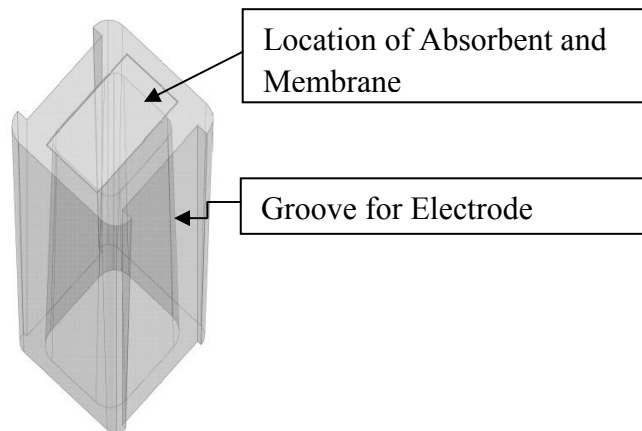
Figure 6. 3-Dimensional Chamber Body
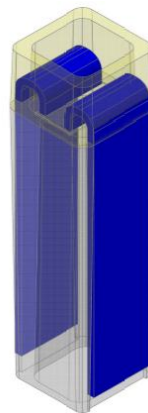
Figure 7. CAD Rendering of a Complete Electrofusion Chamber

22

3.5.2 Fusion Chamber Materials of Construction and Assembly

The chamber body and top were injection molded using Delrin, which is an acetal homopolymer resin. This resin is ideal for engineering applications like this as it will retain its dimensions even when exposed to the high heat environment of an autoclave. The electrodes, as mentioned previously, were made of aluminum. Aluminum is an excellent conductor of electricity as well as heat. The electrodes were stamped out of bar stock. The ends that mated with the porous membrane were finished (inspected and sanded) by hand to make sure that there were no sharp edges that could interfere with the application of electric fields to the cells.

All of the chamber parts indicated in Figures 3 – 7 had to be assembled to make a complete device for use. Devcon® High Strength 5 minute setting epoxy was used to hold the components together. The epoxy was stated to resist water and have a working temperature range from -40°F to 200°F. This epoxy proved to be ideal for electroporation experiments as it provided insulation at electric field strengths higher than 2500 V/cm. Several other brands of epoxy dielectrically broke down in fields greater that 2500 V/cm. Assembled fusion chambers were allowed to cure at room temperature for a minimum of twenty four hours before they were used.

3.5.3 Porous Membrane and Absorbent

Throughout this research study, several porous membranes were investigated for use in the fusion chamber. The pore size and pore density could affect results by altering absorption time of the cell suspension and cell to cell contact on the membrane. Thus the specifications of the membrane were and experimental variable that will be discussed in

23

section 4. Results. However, a Sterlitech™ 0.2 micrometer (μm) pore size membrane was determined to be optimal. This membrane was advertised as hydrophilic with a pore density of 3 x10^8 pores/cm^2. With such a high density of pores, it was theorized that the aqueous phase of cell suspensions would permeate the membrane evenly. This even distribution would ideally leave a cellular paste on the membrane surface with cells in contact to favor high fusion yields. The average size of the cells that were used in this research was approximately 12 μm in diameter. So, cell loss through the membrane was not an issue as the pore size was much smaller than the cell's diameter.

3.5.4 Incorporation of Centrifugation Prior to Electrofusion

Throughout this research study several attempts were made to increase fusion yields using modified methods for inducing cell to cell contact on the membrane surface. One method that differed from the standard of allowing the aqueous phase of the cell suspension to be absorbed through the membrane by an absorbent pad was centrifugation. This method involved placing a cell suspension into each chamber and then centrifuging at 100 RCF at 30°C for one minute.

Chapter 4. Results

4.1 Development of Cell Detection and Quantitation Methods

Fluorescence microscopy was one method used to detect fused cells. This method is semiquantitative in that it required manual counting of visualized cells. In order visualize cells using fluorescence microscopy, the cells had to be stained with fluorescent dyes in order to aid in the detection and quantitation. One red and one green fluorescing stain were used for any particular experiment. Fusion experiments homogenous fusion experiments used the same cell type as partners for fusion. For this type of experiment, half of the cells were stained with a red fluorescing dye and the other half were stained with a green fluorescing dye. Heterogeneous fusion used two different types. One type of cell was stained red and the other green. For both cases, red and green cells were mixed together prior to fusion. Staining was necessary because it would otherwise be difficult to determine if a particular cells resulting from a fusion experiment was a fusion product or unfused cell. The dyes allowed fused cells to be visualized as dual fluorescing whereas unfused cells were either red or green.

Two different combinations of red and green dyes were used in this study for microscopic evaluation of fusion. The first was CMFDA which fluoresces green and CMTMR which fluoresces red, these are described in the Chapter 3. Materials and Methods. The cell types used in this study required different concentrations of CMFDA

25

and/or CMTRM for the staining process in order to produce cells that would be visualized under the fluorescent microscope used in this study. These concentrations are also discussed in Chapter 3. Materials and Methods. The other combination of dyes was DiI which fluoresces green and DiO which fluoresces red. Staining concentrations for these dyes were also optimized for each cell type for microscopic visualization. The staining concentrations and other particulars are provided in Chapter 3. Materials and Methods.

The two sets of fluorescent dyes, CMFDA/CMTMR and DiI/DiO were also used to quantitatively evaluate fusion samples using flow cytometry. Flow cytometers can detect fluorescence at much lower levels that the human eye. Therefore, each cell type required a much lower staining concentration of dye so that they could be detected by the flow cytometer used in this study. The concentrations for each cell type are presented in Chapter 3. Materials and Methods.

Fluorescent microscopy required the development of specific methods, other than the staining, for its use. Similarly, flow cytometry required the development of specific methodology. The resulting methods are provided immediately below.

4.1.1 Microscopy

Fluorescent microscopy was utilized in this research study to optimize dye concentrations to detect homogeneous and heterogeneous fusion. A Leica® microscope (Model DMIL), shown in Figure 8, which was equipped with fluorescent filters that

www.manaraa.com

could detect both green and red fluorescence simultaneously. The microscope was
equipped with a camera that could capture both white light and fluorescent images.
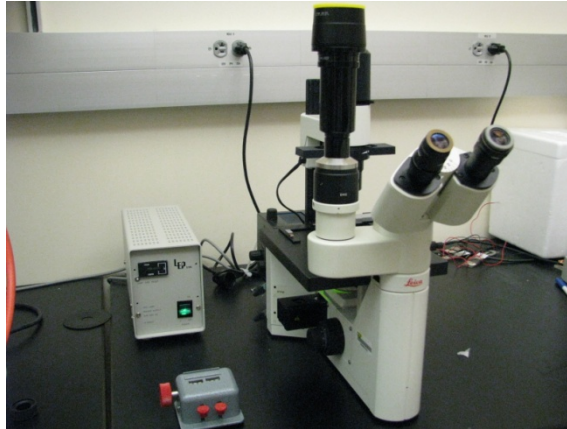
Figure 8 Fluorescent Microscope (Leica® DMIL)

Figure 9 shows images that were acquired using the fluorescence microscope and
camera. Images A and B show B16 cells that were optimally stained for microscopy with
CMFDA and CMTMR, respectively. Figure C shows a 1:1 mix of the CMFDA and
CMTMR stained prior to fusion, and Figure D shows a post fusion dual fluorescent
sample. Many dual labeled hybrids can be seen in D. They appear as having separate red
and green components. They often appear larger in size.

Manual quantitation was conducted using images like those in Figure 9. The
procedure included counting the total number of dual labeled hybrids by the total number
of cells.   An average of 22.3% percent fusion was calculated for the sample shown in
Figure 9D, for example. In addition to dual labeled fusion, single labeled fusion was also
detected. Figure 10 shows and example of this in the form a multiple CMTMR (green)
stained cells that were fused. The image shows a cell in which five distinct nuclei can

27

clearly be detected: There were analogous single labeled fused cells that were made form

only red stained cells.
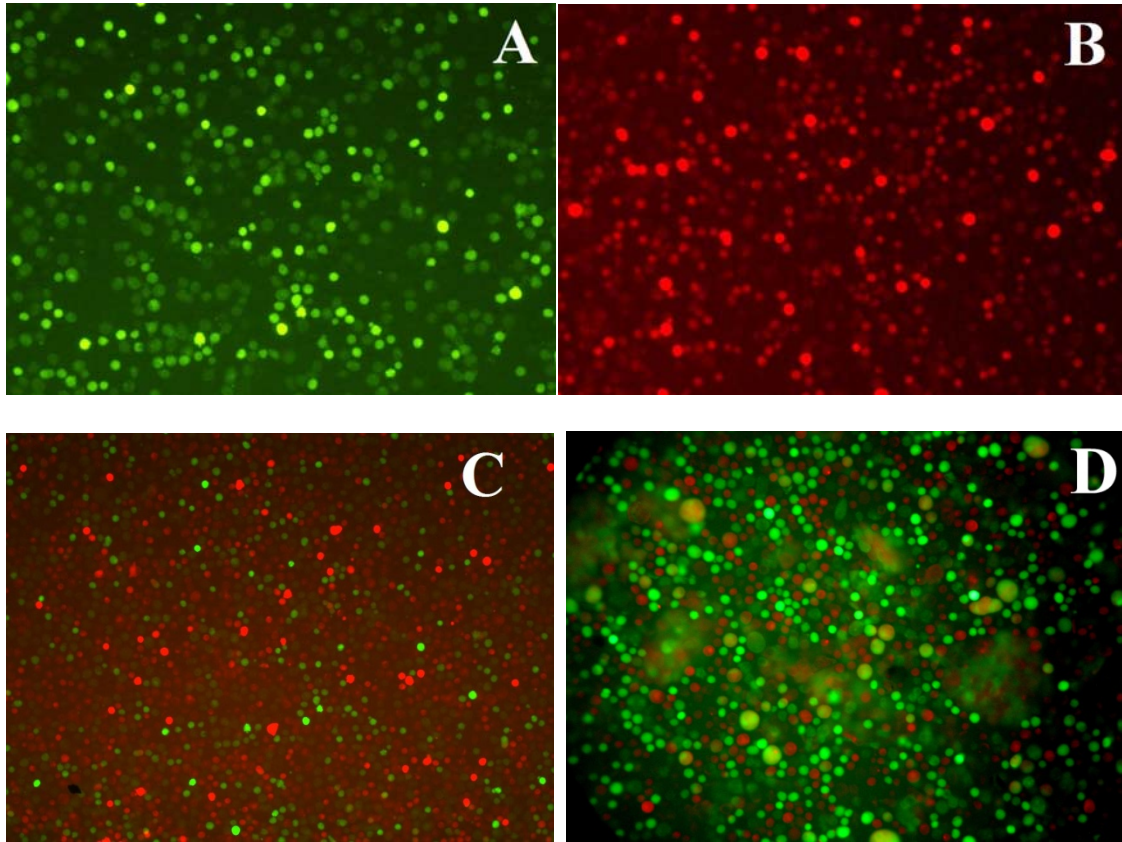
Figure 9. Microscopic Detection of Fused Cells. A) CMFDA Stained B16 Cells, B)

CMTMR Stained B16 Cells, C) 1:1 Ratio of an Equivalent Concentrations and D) Dual

Labeled Fused Hybrids.

28
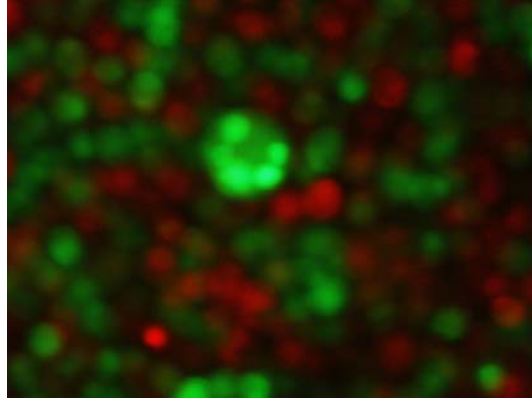
Figure 10. Single Labeled Fused Cells

4.1.2 Flow Cytometry

Flow cytometry is a powerful and dynamic tool used in biological analysis. The
technology is laser based, and scans particles that are directed in a medium flow by a
pressure past a laser beam. As the particles diffract the laser beam, light and fluorescence
are emitted. The emission data is specific to each particle that diffracts the laser beam
and is recorded by a transducer that outputs vital morphological data. This data includes,
but is not limited to size, cell membrane topography, viability, and necrosis. Cell
populations of interest can also be segregated by means of sorting to further characterize
sub populations. The flow cytometer, as shown in the Figure 11, was located in the USF
College of Medicine. Dr. Charles Szekeres was the dedicated operator of the flow
cytometer and assisted with all analysis.

Figure 11 BD LSR II Flow Cytometer

Flow cytometers can discriminate amongst subpopulation of cells within a single sample. For example, flow cytometers can analyze a specified total number of events, or cells from a sample. From this total population, a subpopulation can be identified and quantitated to discriminate what percentage of those cells were green fluorescing, red fluorescing, dual fluorescing, viable, multinucleated, or of a particular size. The same percentage can determined based upon a variety of other biophysical and biochemical characteristics. For this study, flow cytometry analysis focused on the size of the cells resulting from increased cell volume due to fusion and fluorescence. Subpopulations were identified and quantitated not only for dual labeled fusion hybrids, but also for green to green or red to red fusion. Lastly, subpopulations were used to quantitate viable fused cells and nonviable fused cells.

Dye concentrations were optimized due to the sensitivity of the flow cytometer, as previously mentioned. These concentrations resulted approximately equivalent fluorescence magnitudes as shown in Figure 12 acquired from typical experimental controls.
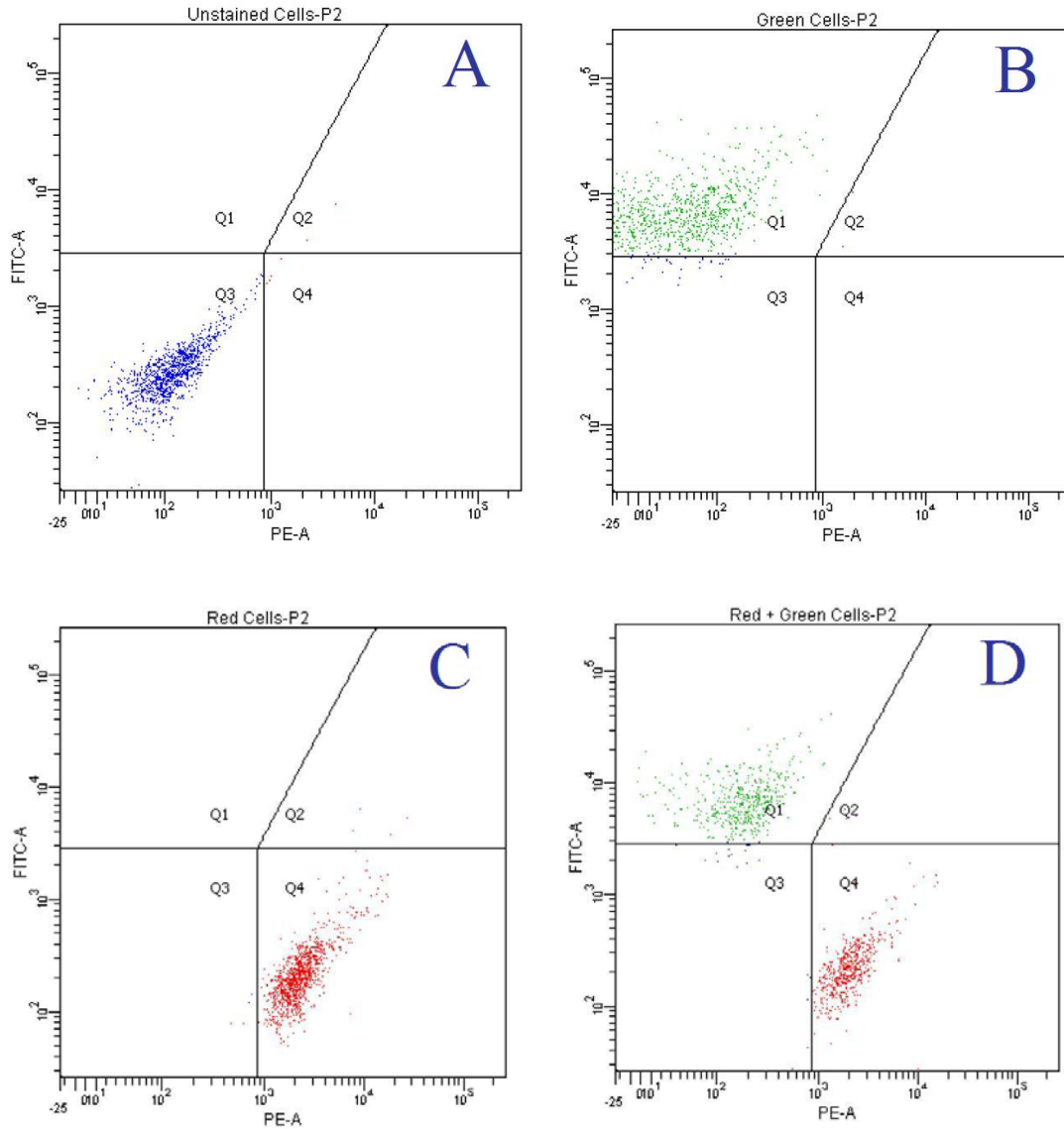
30

Figure 12. Flow Cytometry Scatter Plots from Typical Control Samples. A) Unstained B16-F10 Population. B) CMFDA Stained B16-F10 Population. C) CMTMR Stained B16-F10 Population. D) CMFDA + CMTMR Stained B16-F10 Population.

31

Each of the plots in Figure 12 has a collection of dots. Each dot represents the analysis of a single event or cell. The x-axis is labeled FITC-A in each plot, in Figure 12, which stands for flourescein isothyocyanate and represents the fluorescent magnitude cells detected in the 515-545 nanometers (nm) range. This range was used to detect the green stains used in this study. The y-axis of each plot is labeled PE-A which stands for Phycoerythryn. Cellular fluorescence detected in the 557-599 nm range has a magnitude on this axis. Thus, this range was used to detect red stained cells. This depicts the fluorescence magnitude ($>10^4$) of CMFDA stained B16 cells. Analysis software was used to differentiate these cells into a quadrant labeled 1. Figure B resulted from analysis of CMTMR stained B16 cells. These cells had a fluorescence magnitude of ($>10^3$) in quadrant 4. The final plot shows data obtained from unstained B16 cells which had very low levels of red and green fluorescence.

The control sample dot plots shown in Figure 12 were part of all experiments. The analogous plots for fusion samples were used to discriminate additional sub populations that corresponded to unfused red, unfused green, dual labeled hybrids, and single color hybrids. In order to discriminate all of the possible combinations of fusion products that could be created, refer to Figure 9D, it was envisioned that cell size would be useful. Figure 13A shows a typical plot of forward scatter width (FSC-W) versus forward scatter area (FSC A). This was a plot of cell width/diameter versus cell area. This rectangular region drawn in the figure indicates that larger cells could be discriminates from smaller ones. The viability of fusion products were a concern for this research because a long term goal was to create hybrids for cell transplantation. DAPI (4',6-diamidino-2-phenylindole) is a nucleic acid stain commonly used in conjunction

with flow cytometry and microscopy. The blue stain can be used for both live and fixed cells but can also be used to determine viability. DAPI is selective for nucleic acids Adenine and Thymine (AT) and passes through a live cell membrane much less efficiently than a non-viable cell membrane. The resulting cellular fluorescence can be measured on a dot plot. Then, DAPI positive cells can be discriminated from the total population. Figure 13B shows a plot of viability of all cells in a post fusion sample.
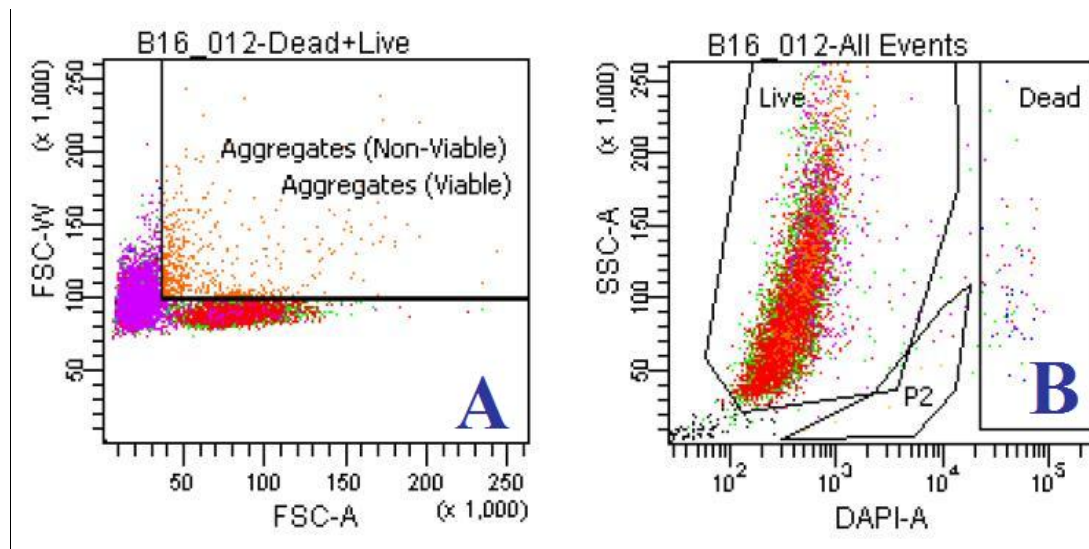
Figure 13. Flow Cytometry Dot Plots for Discrimination of Cell Aggregates and Viability A) Aggregate Cells (Viable and Non-Viable) B) Total Viability and Non-Viability of a Cell Sample using DAPI Nucleic Stain

Flow cytometry data for each sample was output in a convenient table. The data included the number of events counted in the sample, the number of red and green cells, fused dual fluorescent hybrids, viable and non-viable aggregated cells. Table 1 depicts data output from a typical sample. Initially, for each sample, a total population is counted

33

by the flow cytometer. This allows sub-populations to be characterized as a percentage of the total. The sub-populations can be listed directly under the total population or as an additional sub-population for further analysis. The two main sub-populations, as depicted in Table 1, are entitled Live and Dead which directly reflect the sample viability. In this particular sample, the total viability was 90.8 %. Additionally, several sub-populations of the Live and Dead sections were included for further analysis. For purposes of this research, the specific sub-populations that were utilized for calculations included Fused, Fused-1, Aggregates and Aggregates2. Fused was quantitated by the flow cytometer and was indicative of live dual labeled hybrids. Fusion viability was a key factor in this bioengineering research and was discriminated from the total fusion. For purposes of statistical analysis, the non-viable fusion was also quantitated and is illustrated in the table as Fusion-1. Adding the two percentages together would equal the total amount of fusion accomplished for the sample based on fluorescence. It was envisioned that in addition to fluorescence, fusion could be quantitated based on size. Total volume would be increased based on cytometric mixing and could be discriminated by a flow cytometer based on width and surface area, as depicted in Figure 13A. Two overlapping gates were included in the flow cytometer data to produce one sub-plot with two sets of data. The size based fusion was entitled Aggregates and Aggregates2 which reflected viable and non-viable size based fusion, respectively. Utilizing all this information, Table 1 illustrates a total fusion was 20%, while the viable fusion was 13.1%. Subsequent experiments revealed the need to properly align flow cytometry gates to enhance the accuracy of fusion quantitation. For this reason, an optimized protocol

34

was devised so that the results could accurately be reported and duplicated. Experiments

revealed that fusion could be detected by the flow cytometer as shown in Figure 14.

Table 1 Typical Flow Cytometry Output Data

Tube: B16_005

Population	#Events	%Parent	%Total
■ All Events	11,016	####	100.0
■ live	10,000	90.8	90.8
■ Green	2,694	26.9	24.5
■ Red	4,699	47.0	42.7
■ Fused	624	6.2	5.7
■ Aggregates	818	8.2	7.4
■ Dead	8	0.1	0.1
■ Aggregates2	6	75.0	0.1
■ P2	0	0.0	0.0
■ Green-1	2,822	25.6	25.6
■ Fused-1	748	6.8	6.8
■ Red-1	4,741	43.0	43.0

Total fusion and viable fusion were calculated using Equations 5 and 6.

$$Total\ Fusion = (Fused) + (Aggregates) + (Aggregates2) + (Fused - 1) \qquad \text{(Equation 5)}$$

$$Viable\ Fusion = (Fused) + (Aggregates) \qquad \text{(Equation 6)}$$

35
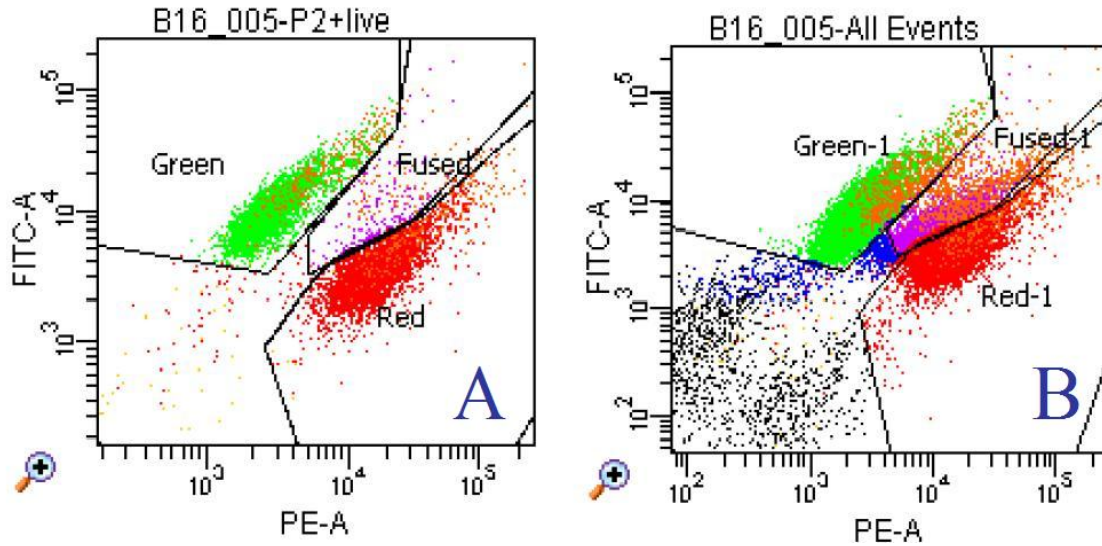
Figure 14. Flow Cytometry Dot Plots of Viable (A) and Non-Viable Fusion (B)

Figure 14A shows a green vs red fluorescence dot plot of a fusion sample. It was constructed to identify dual fluorescing cells using control samples like those shown in Figure 12A-C for reference. Dual fluorescing cells in the plot region labeled fused indicate the location of hybrid cells. The figure was a plot that only showed viable cells, Figure 14B was the same plot with all cells, viable and nonviable, included. These types of plots lead to the standardized construction of plots that the one shown in Figure 15 that had the red and green populations more separated so the fused cells could be more easily differentiated.
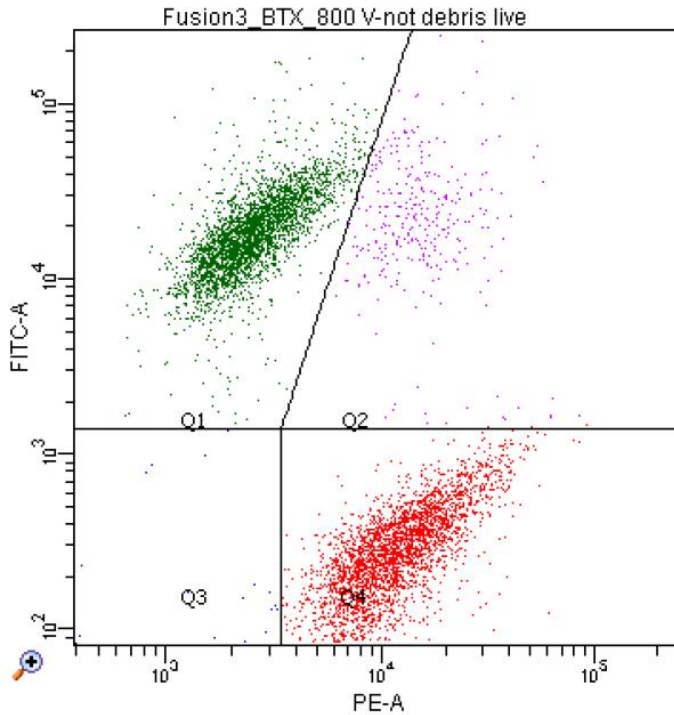
Figure 15. Flow Cytometry Plot of Four Distinct Quadrants

4.2 Characterization of the Fusion Chamber Membrane and Absorbent

4.2.1 Scanning Electron Microscopy

The most critical components of the fusion chamber were the polyester membrane and the absorbent material because these components force cell-cell contact. Therefore, electron microscopy and atomic force microscopy were used to provide a better understanding of these materials before the chamber was tested using living cells. Scanning electron microscopy (SEM) was conducted at the University of South Florida's Nanotechnology Resource & Education Center (NREC). A SEM is used to image the surface topography of a sample with the use of a high energy electron beam. The SEM (Hitachi S-800) used for this study is shown in Figure 16.

37

Figure 16. Scanning Electron Microscope (Hitachi S-800)

The primary goal of this SEM investigation on the membranes was to characterize the surface topography and verify the validity of the manufacturer's stated pore size and density. A smooth membrane would facilitate removing cells from the surface after fusion. The pore size was also a critical characteristic as it should be considerably smaller than a cell diameter so that cells are drawn through the pores and into the absorbent material and consequently unrecoverable post-fusion. Several membranes samples, ranging from 0.2 μm to 10 μm were analyzed.

Sample preparation for SEM analysis included sputter coating each membrane (Hummer X, Anatech LTD). Sputter coating renders a sample electrically conductive because it applies a gold-palladium layer. This layer also protected the sample from the scanning electron beam that is used to generate an image.
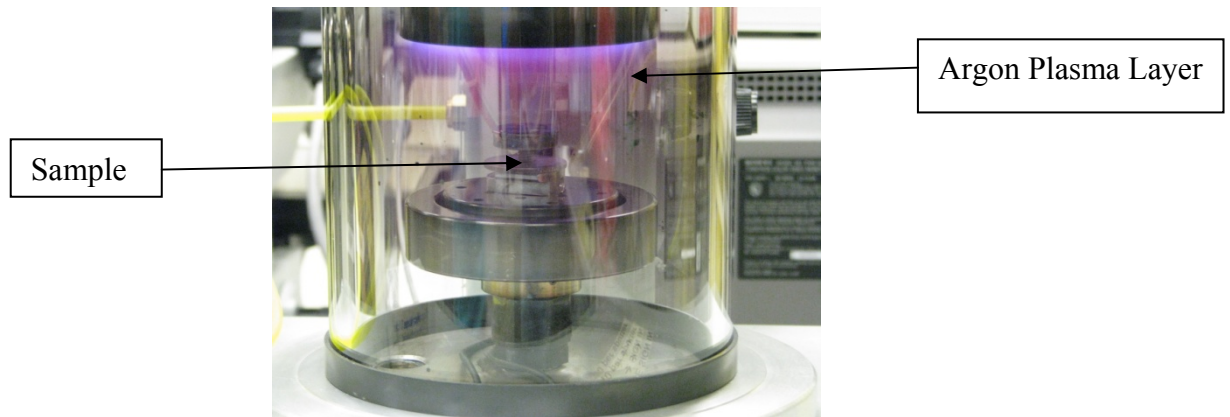
Figure 17. Gold-Palladium Sputter Coater (Hummer X)

Sputter coating uses argon gas under very low pressure to deposit the desired gold-palladium layer. The device was initially purged with 400 millitorr (mtorr) of argon gas. As the internal settings equilibrated, the argon gas was allowed to flow at a constant rate while the pressure remained at 85 mtorr. The constant rate of flow ensured a constant rate of deposition. An ideal deposition thickness is 10-13 nanometers (nm); this required approximately 210 seconds. Once the samples were prepared the electron microscope was used for analysis.

Figure 18 shows images of 0.2 μm pore size polyester Sterlitech membranes. It was theorized that the high density of pores of the 0.2 μm membrane would allow for a more uniform distribution of the cells on the surface. This would enhance cell to cell contact, thereby enhancing fusion. However, during initial attempts, absorption rates were sporadic and inconsistent. The manufacturer indicated that the membrane had a hydrophobic side (visually shiny) and a hydrophilic side (visually matte). The manufacturer also stated that the hydrophilic side should is the preferred side for contact with aqueous solutions. The visual differences were not apparent. Therefore, SEM

39

images were acquired to investigate both sides of the membrane. These are shown in Figure 18. The SEM images confirm the uniformity of both membrane sides.
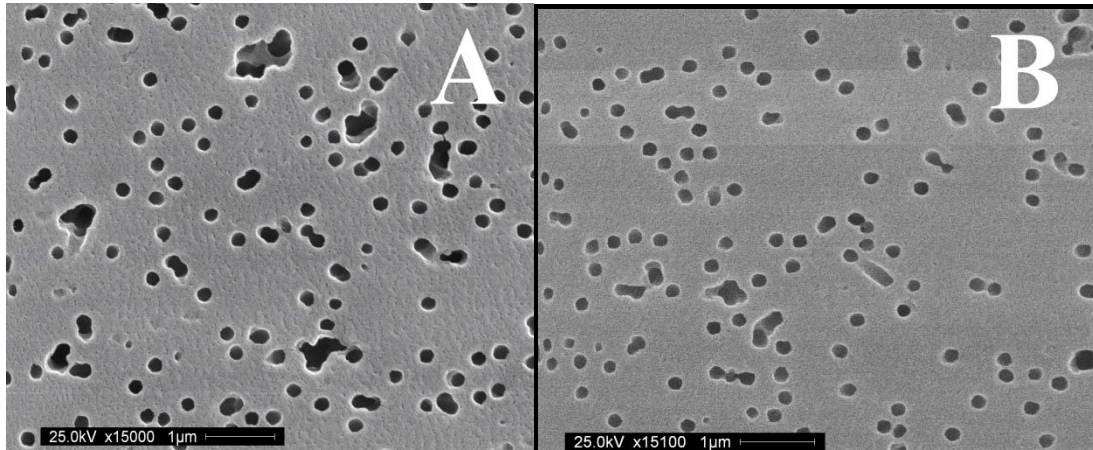
Figure 18. SEM Images of a Sterlitech 0.2 μm Membrane A) Top (x15,000), B) Bottom (x15,100)

Additional polyester membranes were imaged to validate the accuracy of the pore sizes stated by the manufacturer and the smoothness of the surfaces. Figure 19 shows SEM images from 0.6, 5.0, 8.0, and 10.0 μm pore size membranes. Comparison of the bar in each electron micrograph indicates that the manufacturers labeled pore sizes were accurate. Additionally, the membranes were visually quite smooth.

المنارة للاستشارات

www.manaraa.com
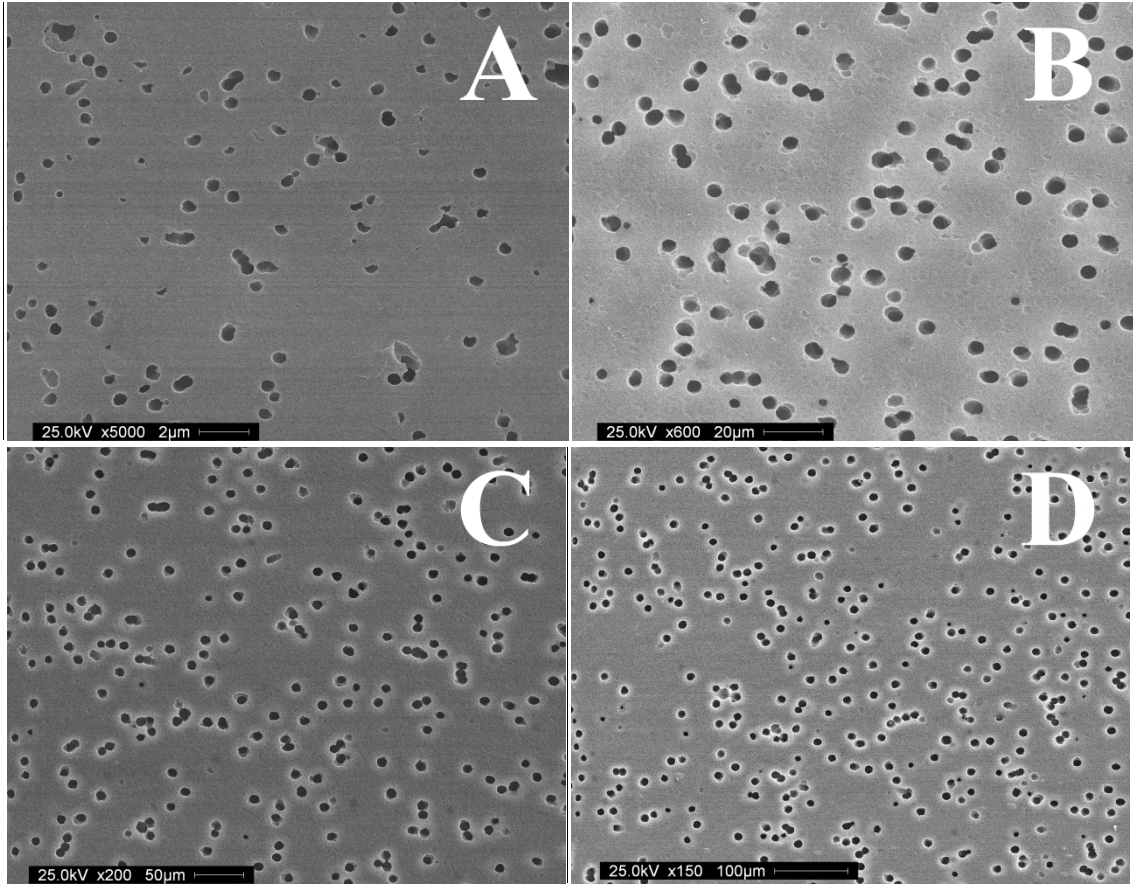
Figure 19 Scanning Electron Micrographs of Polyester Membranes. A) 0.6 µm (x5000), B) 5.0 µm (x600), C) 8.0 µm (x200), A) 10.0 µm (x150)

Figure 20 (A) shows a nylon membrane that had a pore size of 5 µm. This membrane was considered for use in the fusion chamber. However the rough surface revealed by the electron micrograph indicated that it was not well suited for cell fusion. The roughness would most likely retain cells that were deposited onto it. This would make removing fused cells difficult. Figure 20 (B) depicts the absorbent pad which was a woven cellulose material used for industrial filtration. The figure shows an electron micrograph of this material. This material had a thickness of 1.0 mm. Additional tests

41

showed that this cellulose pad was highly absorbent. A 6.7 mm by 10.7 mm piece was required to fit into the fusion chamber. It was determined that a piece of absorbent this size could absorb 0.076 ml (76 µl) of water.
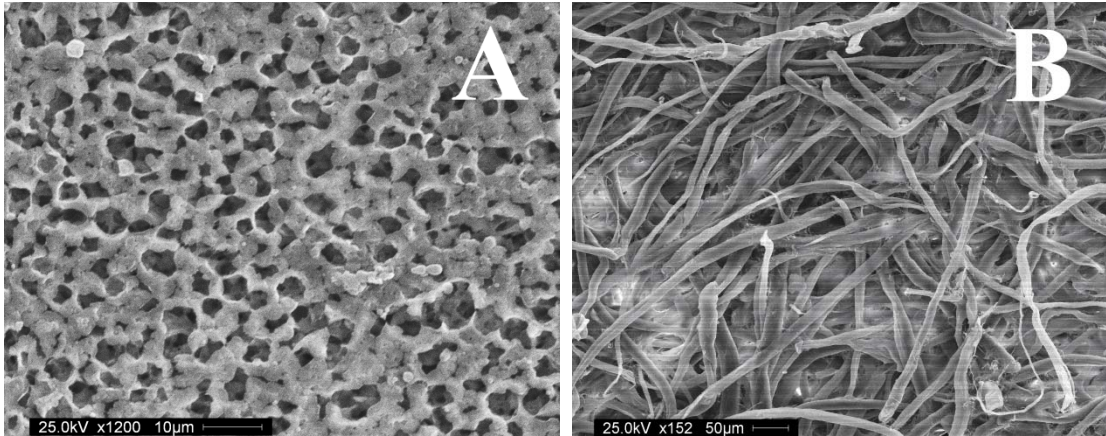
Figure 20. Scanning Electron Micrographs A) 5.0 µm Nylon Membrane (x1200), B) Woven Cellulose Absorbent Pad (x152)

4.2.2 Atomic Force Microscopy

Atomic force microscopy (AFM, PSIA XE-100 Advanced Scanning Probe Microscope) was also used to study the surface topography and three dimensional characteristics of the membranes. The work was accomplished in the University of South Florida's Silicon Carbide Lab. The AMF is depicted in Figure 21.
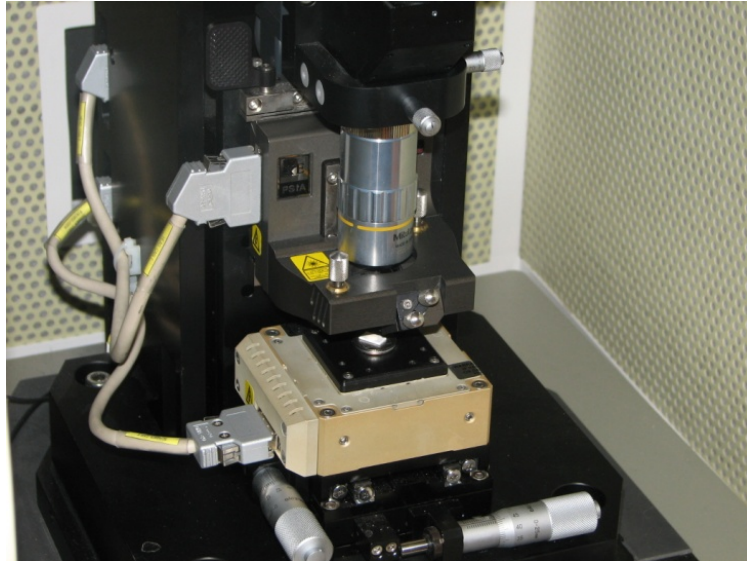
Figure 21. Advanced Scanning Probe Microscope (PSIA XE-100)

AFM is a useful tool in sample analysis and can measure a multitude of forces such mechanical contact forces, van der Waals forces, electrostatic and magnetic forces. The AFM analysis is based on the deflection of the cantilever tip arising from forces when being brought into close contact with the sample. This analysis provided invaluable, three dimensional, topographaphic information regarding both the polyester and nylon membranes.

المنارة للاستشارات

www.manaraa.com
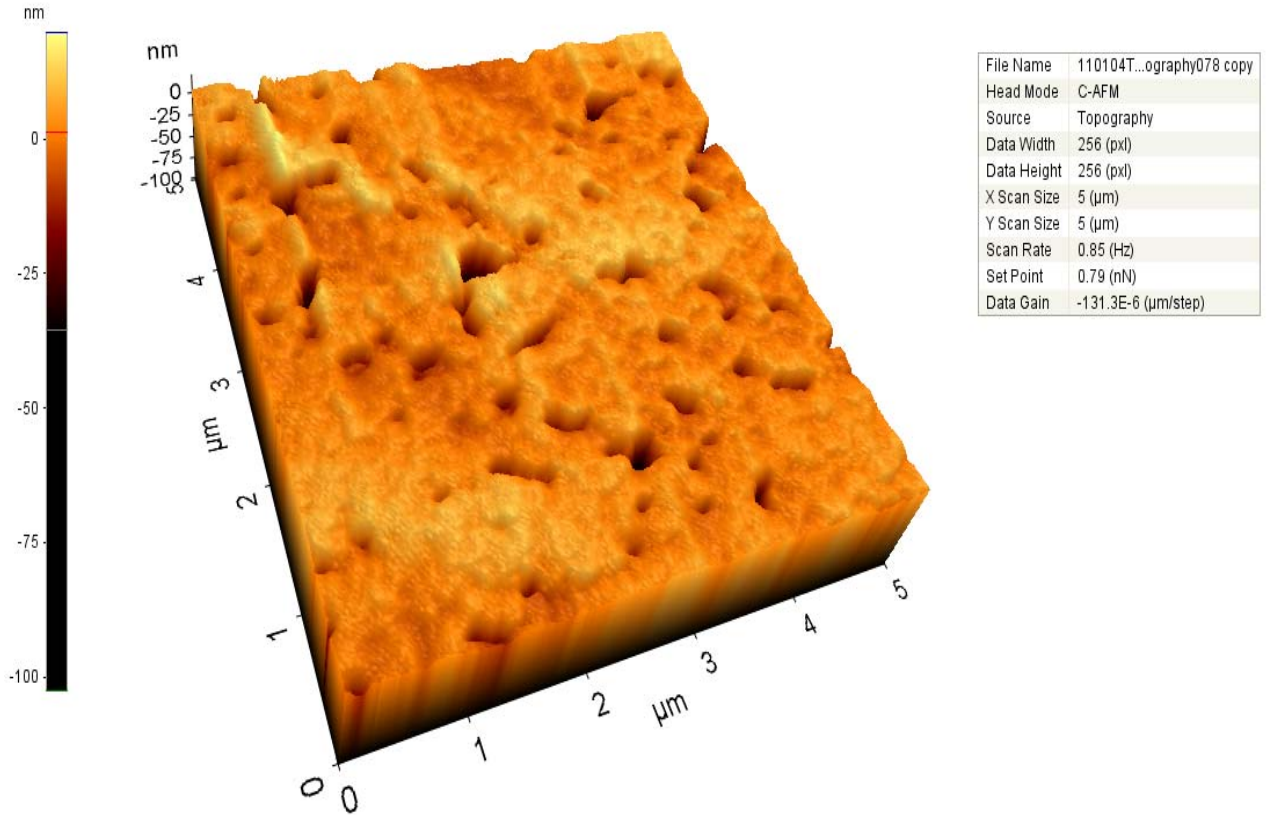
Figure 22. AFM Image of a 0.2 µm Polyester Membrane

Figure 22 illustrates the smoothness of the 0.2 µm polyester membrane. The scale in the

image represents relative depth, measured in nanometers (10^{-9}), in accordance to color.

The lighter colored areas represent regions that are closer to the surface and the darker

colored regions represent the depth of the pores in the sample. This type of surface

topography would be ideal for removing cells and further validated the investigation of

which membrane to use. Figure 23 illustrates the verification of the 0.2 µm polyester

membrane pore size. It was important to validate this measurement prior to the

completion of biological studies as a second quantitative check on the pore size. The red

rectangular size bar in the topographical view of the sample in Figure 23 has two distinct

regions, marked by two red triangles and two green triangles. The triangles were placed during analysis to measure two individual pore sizes. The pore sizes are displayed in the cursor statistics box. The red triangles measured a pore size of 0.293 µm and the green triangles measured a pore size of 0.211 µm. The average of the two measurements was 0.252 µm and was sufficiently accurate for this research.
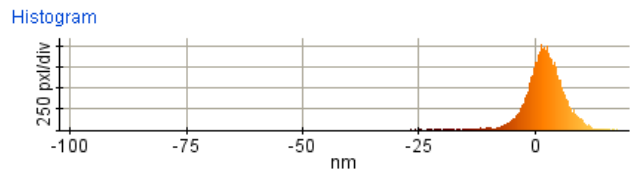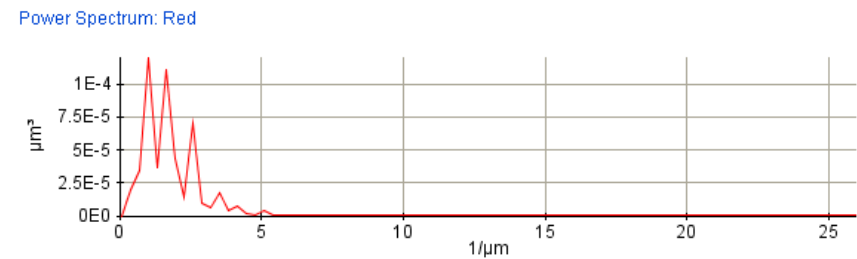
Figure 23. AFM Image from a 0.2 μm Pore Size Polyester Membrane for Pore size Verification

File Name	110112Topography033
Head Mode	C-AFM
Source	Topography
Data Width	256 (pxl)
Data Height	256 (pxl)
X Scan Size	45 (μm)
Y Scan Size	45 (μm)
Scan Rate	0.49 (Hz)
Z Servo Gain	0.43
Set Point	0.68 (nN)
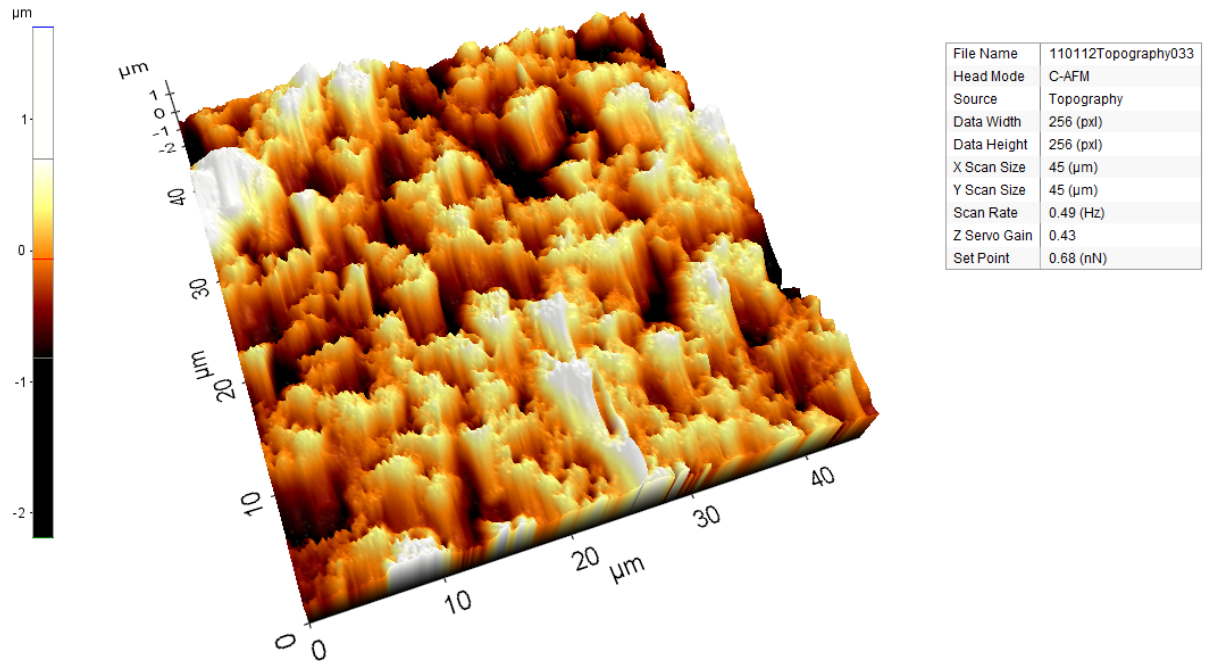
Figure 24. AFM Image of a 5.0 μm Nylon Membrane

In addition to characterizing the polyester membrane, AFM was also used to portray topographic characteristics of the 5.0 μm nylon membrane for comparison. Figure 24 illustrates the roughness of the 5.0 μm nylon membrane. This type of surface topography would increase the difficulty of removing cells and would not be an ideal candidate for this research study. Figure 25 shows verification of the 5.0 μm nylon membrane pore size which was calculated to be 4.842 μm. This determination was accomplished using the same method as for the polyester membrane.
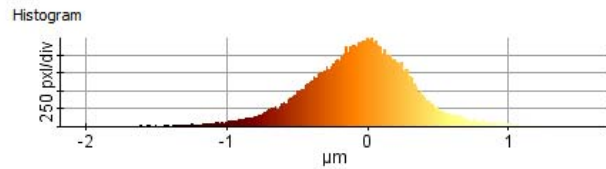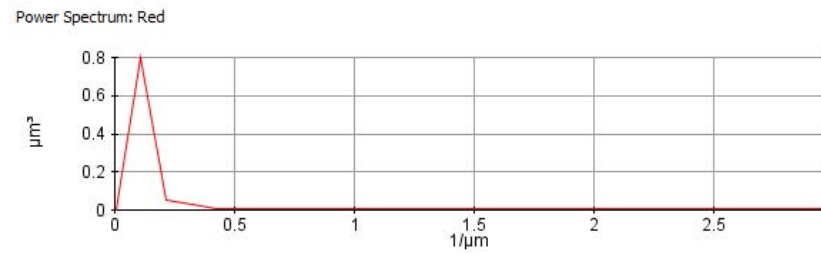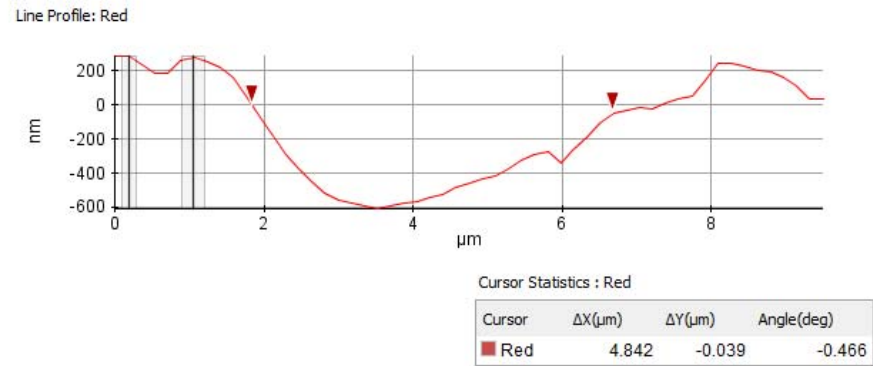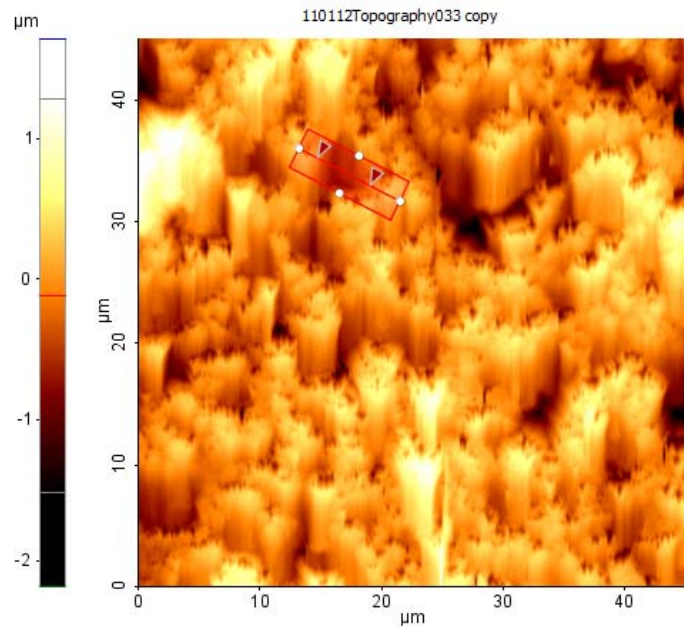
47

Figure 25. AFM Image from a 5.0 μm Pore Size Nylon Membrane for Pore Size Verification

4.3 Development of a Basic Protocol for Using the Fusion Chamber

After developing detection/quantitation methods and characterizing the membranes/absorbent, chamber assembly was addressed as a first step toward using the chamber. First attempts at assembling the fusion chamber revealed that using epoxy to assemble all the parts was not a trivial task because the finished product had to be sealed well enough to hold liquid. Liquid was observed to be drawn by capillary action into all interfaces between the aluminum electrodes and Delrin as well as any air spaces between parts of the chamber. This would ultimately translate to cell losses during fusion. This meant that epoxy had to be used with considerable expertise to seal every avenue for liquid to escape. After a technique was developed to assemble the chambers using epoxy, the quantity of cells to deposit onto the membrane had be determined before testing the chamber.

4.3.1 Absorption Time Optimization with Varying Membranes

In addition to minute details of the cuvette build, the number of cells to deposit onto the porous membranes of each chamber had to be optimized. The goal of this was to introduce enough cells into the chamber so that they would deposit in one or more layers on the membrane to facilitate contact. Since cells would be introduced into the chamber in suspension, it was also important to determine a volume of liquid phase that that these cells should be suspended in. This liquid phase was important as it could not exceed the capacity of the absorbent. Finally, as a practical matter, the time required for the cells to deposit should not be more than several minutes. An experiment was conducted to

49

optimize absorption times for two membranes with different pore sizes as an example of the types of experiments that were performed. For this experiment, the chambers were constructed without the tops. This did not alter the geometry or function of the chamber, but it allowed the membrane to be observed. This judging when all of the liquid was absorbed much easier. Table 2 shows the resulting times required for complete absorption of the liquid from the quantity of B16 cell suspension introduced into the chamber. A fixed volume of 50 µl was used as this was less than the 76 µl maximum capacity of the absorbent used in the chamber.

Table 2 Absorption Time Optimization

Trial	Pore Size(µm)	Concentration (cell/50µl)	Absorption Time (min)
1	0.6	400,000	13.05
2	2.0	400,000	17.53
3	0.6	200,000	5.29
4	2.0	200,000	6.30
5	0.6	200,000	7.38
6	2.0	200,000	10.12
7	0.6	200,000	3.55
8	2.0	200,000	6.10
9	0.6	200,000	4.15
10	2.0	200,000	6.31

As seen in trials 1 and 2, a cell concentration of 400,000 cells/50µl resulted in times greater than 10 minutes. This was far too long to be practical. The quantity of cells was decreased by 50% to 200,000 cells/50µl aliquot. Absorption times were decreased (trials 3-10). The average absorption time for the 0.6 µm pore size membrane was 5.09 minutes (1.69 SD), and the average time for the 2.0 µm membrane was 7.21 minutes

50

(1.94 SD). Preliminary studies were performed on other size and type membranes such as polylcarbonate track etch products and nylon membranes. No dramatic improvements in absorption times were observed. It was possible that the membranes were not as porous, hydrophilic and uniform in nature as advertised. Or, the problem may have been as simple as the cells obstructing the pores and thereby retaining the solution. Subsequent experimentation revealed that there was little difference in absorption time for polyester membranes with pores sizes of 2 μm or less. Therefore, 0.2 μm pore size membranes were used for the remainder of this study. This size was chosen over the others as the pore density was 3×10^8 pores per cm^2 which was the highest pore density available.

4.3.2 Fusion of B16 Cells to B16 Cells

B16 cells were fused to B16 cells after identifying that 0.2 μm membrane and 200,000 cells in 50 μl would be used for all fusion. B16 cells were grown, stained for flow cytometry, harvested, enumerated and otherwise prepared for fusion experiments as described in 3. Materials & Methods. Fusion was conducted with half of the B16 cells stained with CMFDA and the other half stained with CMTMR. Figure 26 depicts the results of flow cytometry analysis of total and viable cell fusion of nine samples at three separate electrical parameters. The first three samples were pulsed with an electrical field strength of 2000 V/cm, 300 μs pulse length, 8 pulses and a 1 second pulsing interval. The statistical mean total fusion yielded 14.5% ± 3.3 SD, with 4.0 ± 2.3 SD viable fusion. Additionally, the second three samples were pulsed with an electrical field strength of 2250 V/cm, 300 μs pulse length, 8 pulses and a 1 second pulsing interval. The statistical

mean fusion for these three samples yielded 15.9% ± 5.6 SD, with 2.9 ± 0.4 SD viable

fusion. The last three samples were pulsed with an electrical field strength of 2500 V/cm,

250 μs pulse length, 8 pulses and a 1 second pulsing interval. The statistical mean fusion

for these three samples yielded 18.9% ± 8.1 SD, with 2.6 ± 1.4 SD viable fusion. The

successful accomplishment of cell electrofusion showed promise but also indicated the

need to optimize parameters due to low fusion viabilities in comparison to total fusion.

In addition to determining the total and viable fusion, negative control samples, labeled

as No Pulses, as seen in Figure 26, were also collected. This data was vital and

represented samples that were treated in the same manner as other trials but did receive

electrical pulsing. The collection of this data allowed for an accurate depiction of cell-

cell fusion. For each fusion experiment, negative control samples that did not receive

electrical pulsing were collected in triplicate, averaged and illustrated in conjunction with

the standard deviation. The experiment demonstrated in Figure 26 resulted in an overall

average of 1.1% ± 0.8 SD.
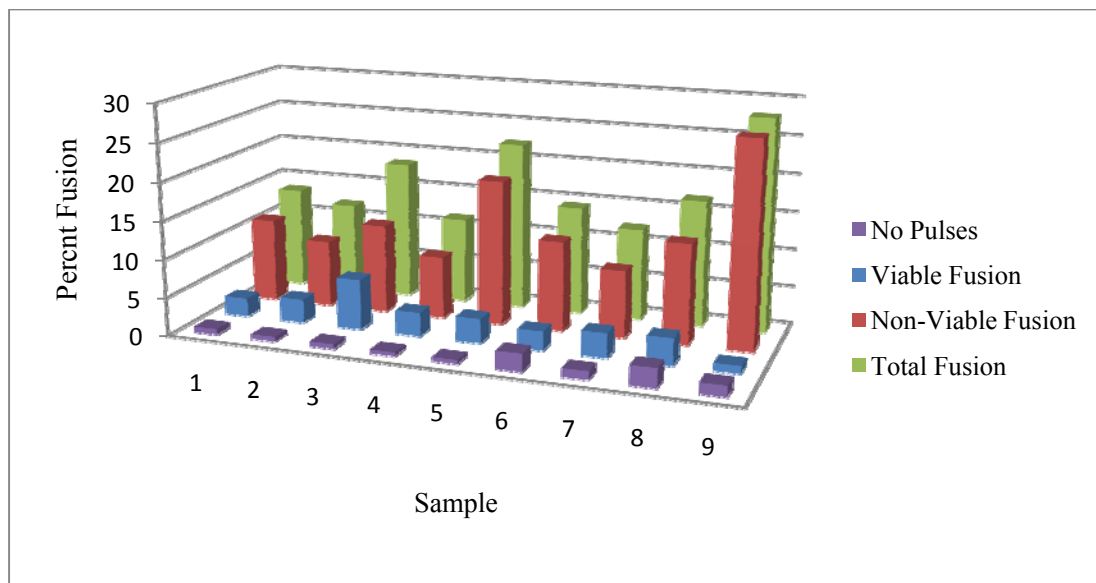
Figure 26.   B16 to B16 Fusion Results Quantitated by Flow Cytometry

www.manaraa.com

4.4 Fusion of Cell Lines

   4.4.1 HaCaT Human Keratinocyte Cells

   After determining how the fusion chamber should be used with B16 cells, fusion was attempted using HaCaT to determine if the chamber could be applied to other cell lines. The HaCaT cell line was stained with CMFDA and CMTMR. These dyes were stained and prepared for fusion in the same manner as described in Section 3 Materials & Methods. One complicating factor that arose with the HaCaT cells was during the trypsinization process used to remove the stained cell monolayers from tissue culture flasks. Trypsinization required 10 – 15 minutes (0.05% Trypsin) at 37°C. The process was long compared to most cell lines. HaCaT cells are derived from epithelial tissue and contain e-cadherins, which are a class of type-1 transmembrane proteins. The "e" stands for epithelial and cadherins are calcium dependent. These proteins are vital in cell adhesion and ensuring the cells within the tissue stays bound together. It was likely that they were the reason for the difficulty during trypsinization which was observed by the presence of cell clumps. They are also the likely reason for related difficulty in achieving a single cell suspension after trypsinization. It should be noted that longer trypsinization periods did produce a single cell suspension. Cells that could not be trypsinized were scraped from the culture flask growth surface. The mean viability for this cell line for the experiments performed was 86.1%. This is slightly lower than what was typically obtained for other cell lines. The reduction was most likely due to the longer trypsinization period and scraping. Fusion was performed by mixing equal numbers of CMFDA and CMTMR stained cells together. Chambers constructed using 0.2 µm pore sized membranes were loaded with 200,000 cells in 50 µl.

www.manaraa.com

4.4.1.1 Microscopy

Fluorescent microscopy was used to visualize fusion of the HaCaT cell line. In each experiment, staining of the control samples was confirmed. This included both the green stained HaCaTs and red stained HaCaTs as well as an equal mix of green and red stained cells. Fusion samples were also examined. Figure 27A shows a CMFDA (green) stained sample as an example. This figure shows the cell clumping what was described above. Figure 27B shows a fusion sample with a large fused cell comprised of green cells only. This was a commonly observed type of cell. It indicated that clumps of cells may be fused in the chamber. Figure 28 shows a very large cell that clearly contains both red and green stained cells. There is evidence of some fusion; however, it is not clear how much. It was also a common occurrence and was most likely due to the tendency of this cell line to clump. The photos in Figures 27 and 28 were acquired using a microscope in the Cell and Pathology Laboratory of Dr. Don F. Cameron, USF College of Medicine.
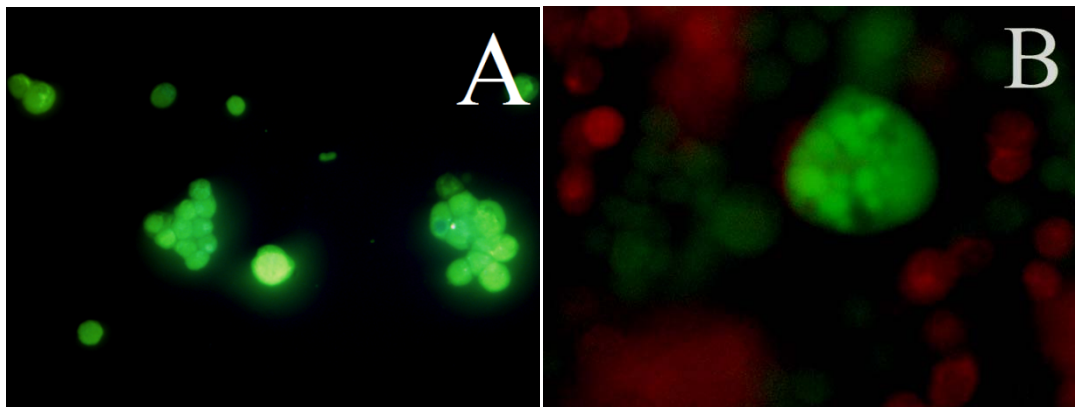
Figure 27. HaCaT CMFDA Cell Samples A) Control Sample B) Fusion Sample

www.manaraa.com
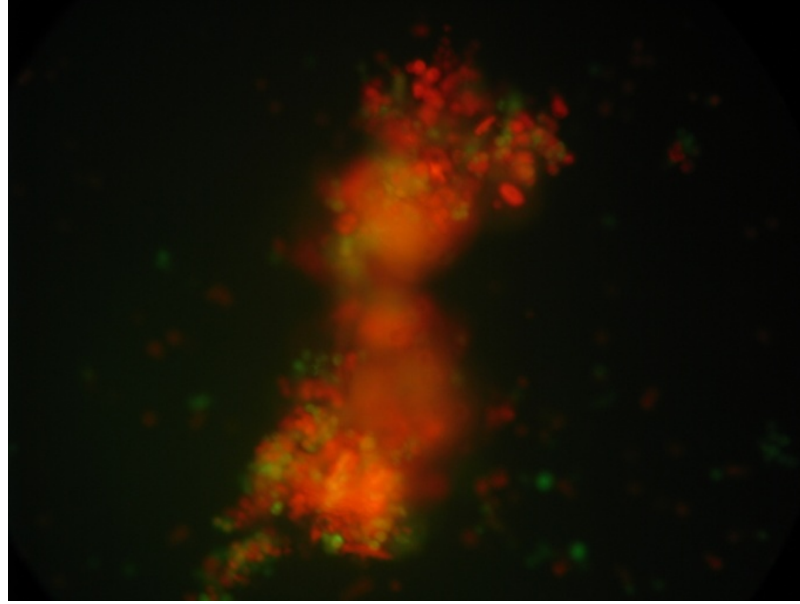
Figure 28 HaCaT Cell Clumping

4.4.1.2 Flow Cytometry

Flow cytometry analysis was accomplished in the same manner as described for the B16 cell line, above, and in 3. Materials & Methods. However, final dye concentrations for CMFDA and CMTMR were optimized at 1.70 µl dye/50 ml medium and 17.0 µl dye/25 ml medium, respectively. Fluorescence control plots for CMFDA and CMTMR stained HaCaT cells were acquired, and the samples were analyzed for the presence of fusion in reference to their controls.

Flow cytometry results from the fusion of the HaCaT cell line and resulted an average initial viability of 92.3% (STD 7.5) from unfused control samples. Electrofusion parameters, complicated in triplicate, were 2000, 2250 and 2500 V/cm. All samples received 8 pulses with varied pulse lengths that were between 250-300 µs. Figure 29

55

shows the results. These results showed relatively high fusion yields. These should be taken into account with the fluorescent microscopy results shown above as clumping was most likely present. This degree of clumping would make analysis of flow cytometry results difficult.
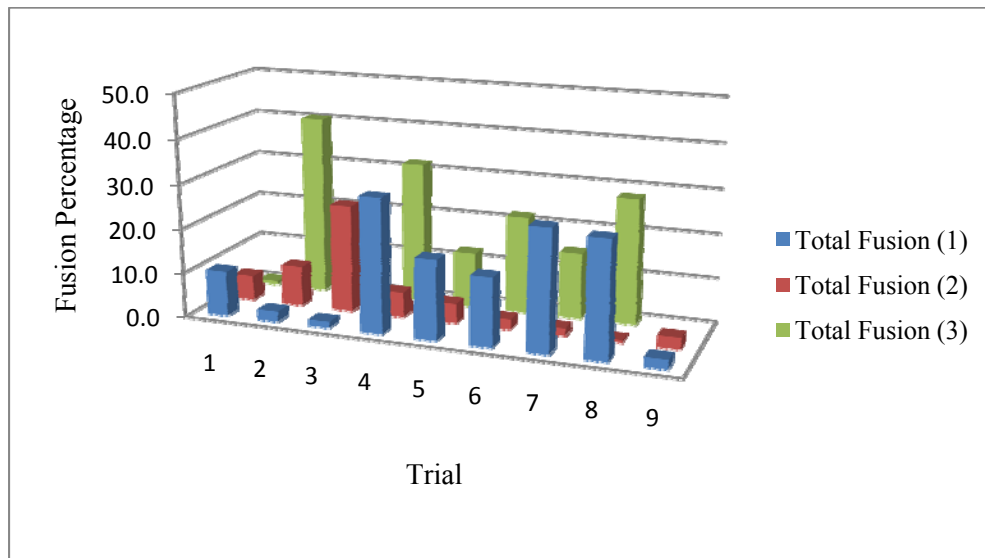
Figure 29 HaCaT Fusion Results Quantitated by Flow Cytometry

4.4.2 H4 Neuroglioma Cells

The H4 cell line was fused as another example cell line to investigate the utility of the fusion chamber. The H4 cells were morphologically similar to the HaCaT cells. They were also difficult to trypsinize, and required 10 – 15 minutes exposure to trypsin at 37°C (0.05% trypsin). H4 cells contain N-cadherin which would produce the same cell adhesion effect observed with HaCaT cells. The cell detachment was verified using a microscope and a cell scraper was used to dislodge any remaining attached cells

4.4.2.1 Microscopy

The H4 cells were stained using 25 µl of CMFDA and 45 µl of CMTMR per 12 ml of medium in 80% confluent 75 cm^2 polystyrene cell culture flasks. Fluorescent microscopy was utilized once again to observe fusion. For each experiment, control samples were observed to confirm the green stained, red stained, and 1:1 mixtures of green and red stained cells. Figure 30A shows a typical control sample that was stained with CMTMR. Note that there are single cells, but there are also many cells that are adhering to one another. Figure 30B shows a post fusion sample. Fused cells presenting both single and dual fluorescence were frequently observed. However, there were also may cell clumps that contained both red and green stained cells. The images were acquired in the Drug & Gene Delivery Lab.
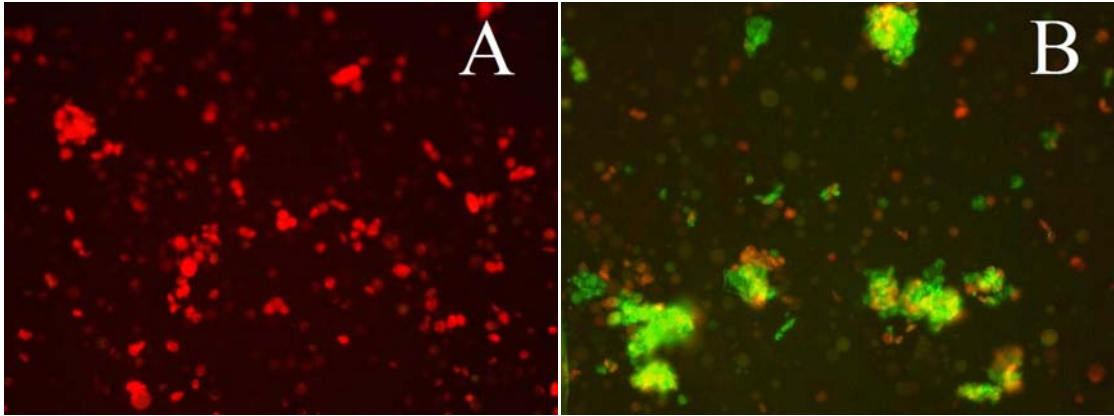
Figure 30   H4 Cells. A) CMTMR Stained H4 Control. B) Dual Labeled H4 Hybrids.

4.4.2.2 Flow Cytometry

Dye concentrations for samples that were analyzed by flow cytometry were 1.5 μl CMFDA dye/50 ml medium and 13.5 μl CMTMR dye/50 ml medium. Flow cytometry analysis was performed on control and fused samples as described in 3. Materials & Methods. The first three samples were pulsed with an electrical field strength of 1500 V/cm, 300 μs pulse length, 8 pulses and a 1 second pulsing interval. The statistical mean total fusion yielded $4.6\% \pm 4.8$ SD. Additionally, the second three samples were pulsed with an electrical field strength of 2000 V/cm, 300 μs pulse length, 8 pulses and a 1 second pulsing interval. The statistical mean fusion for these three samples yielded $21.0\% \pm 7.9$ SD. The last three samples were pulsed with an electrical field strength of 2500 V/cm, 300 μs pulse length, 8 pulses and a 1 second pulsing interval. The statistical mean fusion for these three samples yielded $18.3\% \pm 14.1$ SD. Cell clumping was viewed as a potential confounding factor for flow cytometric analysis. Thus the fusion of the H4 cell line in the chamber was not pursued further.

58

4.4.3 Human Sertoli Cells

Human Sertoli Cells (HSC) were fused as yet another example cell line. These cells were not isolated from human hosts during this research. They were once primary cells that were immortalized by a proprietary means. The primary cells were isolated from human cadaveric testes between the ages of 12-36 years (Chui, Trivedi et al. 2010). They were provided to the Cell & Pathology Lab by Dr. Constance John (Mandel Med, Inc.; California). Figure 31 shows a confluent culture of the HSC line under white light. Figure 32 shows the cells after trypsinization and shows the spherical structure of the cells. The average diameter of these cells was approximately 20 µm.

Figure 31 Human Sertoli Cells (Plated)
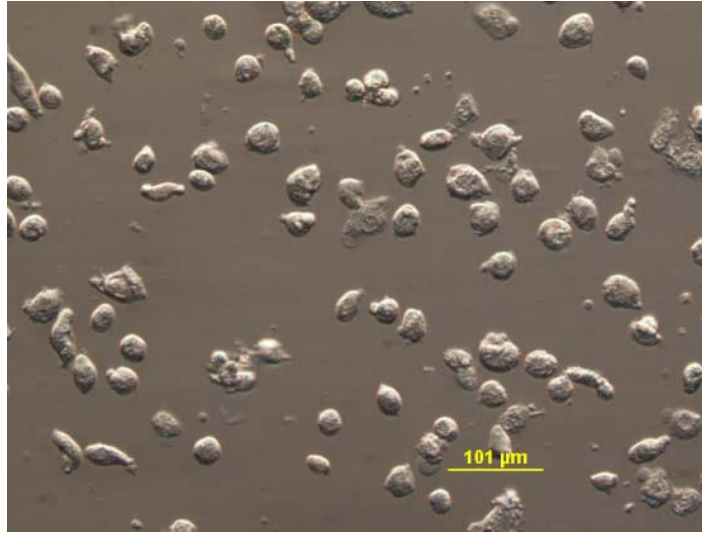
Figure 32 Human Sertoli Cells (Post Trypsinization)

4.4.3.1 Microscopy

The lipophilic stains DiL and DiO were used for this experiment both at
concentrations of 4µl/ml. Figure 33 shows CMTMR and CMFDA stained human sertoli
cells that were used as control samples. Four separate fusion attempts were made
experiment using cells like those shown in the figure. Four samples were electroporated,
two with a field strength of 1500 V/cm and the other two 2000 V/cm. All four samples
had a 300 µs pulse length, 8 pulses and an interval of 1 second between pulses. The goal
of this study was to demonstrate fusion of a novel cell line. Figure 34 shows an example
of the products of fusion. The goal was also to reseed electrically treated cells to
determine their ability to survive in culture. The cells were provided with fresh medium
after fusion and survived only 4 days post electrical treatment. The cells did not show
any evidence of proliferation but did initially attach to the culture flask.

60
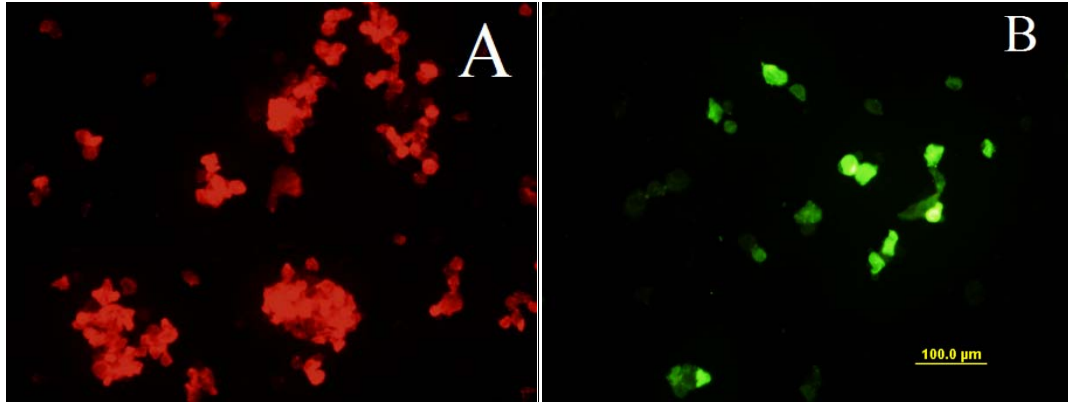
Figure 33 Stained Human Sertoli Cells. A) CMTMR stained control. B) CMFDA stained control.
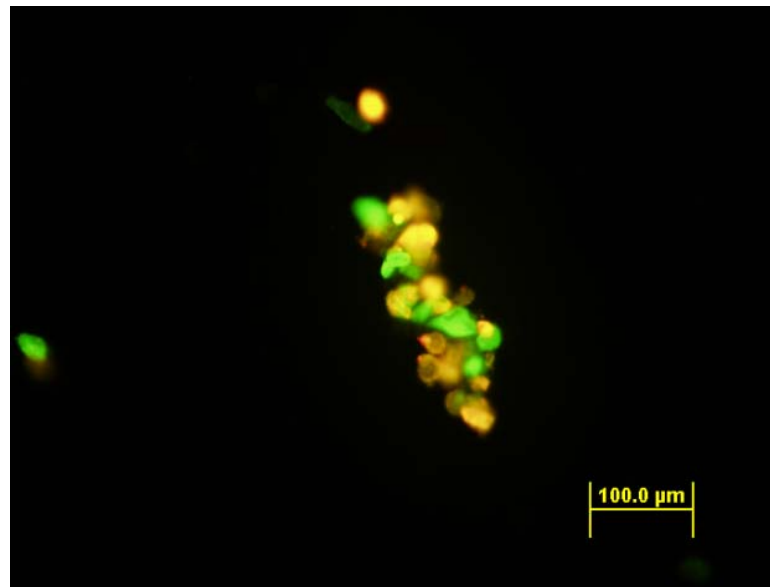
Figure 34 Human Sertoli Cell Fusion

61

4.4.4 HSC and B16 Heterogeneous Cell Fusion

Throughout this research the same a single type of cell was used for fusion. This meant that hybrids were two or more cells of the same type. Although this was convenient for examining the utility of the fusion chamber, it was an artificial example. For a hybrid cell that would have utility from a scientific or medical standpoint should be comprised of two different cells that when combined create a cell with novel characteristics. As an example of heterogeneous fusion, B16 and HSC cell lines were fused. The B16 cells were stained with 30 µl of CMFDA in 12 ml of media, and the HSC cells were stained with 30 µl of CMTMR in 12 ml of media. Both cell types were stained in their respective supplemented mediums for 30 minutes at 37°C. Three samples were fused with a field strength of 1500 V/cm, 8 pulses and a 300 µs pulse length. Fused samples were readily seen during evaluation and are depicted in Figure 35.
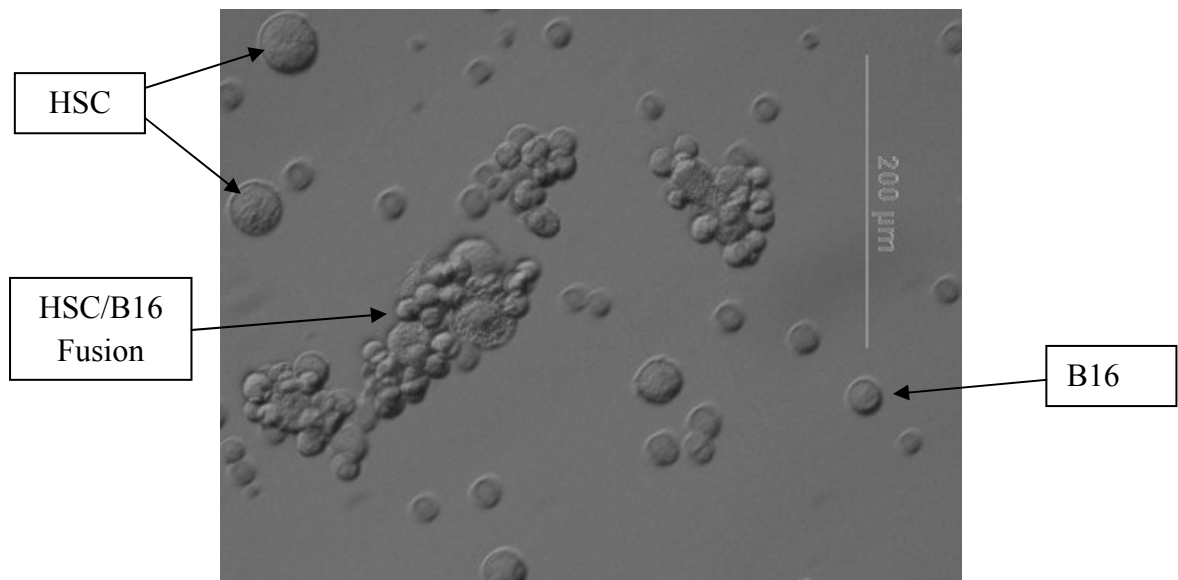
Figure 35 Human Sertoli Cell/B16 Cell Fusion

Within the field of view in Figure 35, successful fusion was accomplished as indicated by the arrows and labels. B16 cells do not exhibit the type of cell clumping that was noticed in the HaCaT and H4 cell lines. Additionally, the HSC were not clumped together as also observed above. The numerous aggregated cells suggest in Figure 35 are a novel fusion cell construct and showed promise for future research studies. The reason that these hybrids show promise for the future of the fusion chamber is that they are a heterogeneous hybrid. More specifically, human Sertoli cells have immunologic effects when transplanted into a host that prolong survival. Therefore, Sertoli cells fused to other cell are a means for ensuring the survival of transplanted cells.

4.5 Centrifugation as an Improved Cell to Cell Contact Method

During this thesis research, it became apparent that centrifugation may be an effective means for forcing cells in the chamber to deposit onto the polyester membrane. This required no modifications to the fusion chamber and when employed would essentially add centrifugation as an additional cell contact method. Thus cells would be charged into the fusion chambers and the absorbent would draw cells onto the membrane. This would be followed by centrifugation as an additional means for forcing cell to cell contact. The cuvettes fit inside a standard centrifuge tube holder for a 15 ml centrifuge tube. Consequently, this method could be applied in any biological lab. Centrifugation has been used by others as a means for achieving cell to cell contact. Other methods included centrifuging the cells prior to applying the electrical pulses (Rols, Dahhou et al. 1994). This method proved to be very useful in this research and has sparked ideas for design manipulation of the fusion chamber.

B16 cells were stained with 25 µl of CMFDA and 45 µl of CMTMR, respectively. The standard protocol for using the chamber was used. This included introducing 400,000 cell contained in 50 µl of solution into chambers that had an absorbent pad and a 0.2 µm membrane. Chambers were centrifuged at 10, 50, and 100 RCF at 30°C for 1 minute. Three samples were centrifuged using each RCF. The 100 RCF samples all resulted in a thick cellular paste suggesting cell to cell contact and sufficient absorption. The other samples appeared to have larger amounts of liquid mixed in with the cells.

Given the apparent success of using 100 RCF to help force cell to cell contact, the standard number of cells placed into the chamber was examined again. This standard number was 400,000 cells in 50 µl. It was derived for one cell monolayer based on the

www.manaraa.com

surface area of the membrane between the electrodes and the surface area of a sphere and assuming a perfect sphere packing factor of 0.74. Equations 7-10 were used to calculate the surface area of the rectangular shaped membrane the circle representing the largest diameter of cell assuming a 10 μm cell diameter.

$$Area_{membrane} = Surface\ Area = L\ x\ W \qquad\qquad \text{(Equation 7)}$$

$$Area_{membrane} = (8.9\ mm)x(4.7\ mm) = 41.83\ mm^2 \qquad\qquad \text{(Equation 8)}$$

$$Area_{circle} = Cross\ Sectional\ Area = \pi\ x\ r^2 \qquad\qquad \text{(Equation 9)}$$

$$Area_{circle} = \pi\ x\ (5\ \mu m)^2 = 79\ \mu m^2\ ) \qquad\qquad \text{(Equation 10)}$$

Therefore, the chamber had 41.83 mm^2 available for cell deposition, and each cell would occupy 79 μm^2. If the cells were perfectly packed in a monolayer with absolutely no void space between them, then the packing factor would be 1.0. Equation 11 shows this calculation, and 529,494 cells would be needed to create a monolayer of cells on the membrane. It is not valid to assume that that there would be not void space between cells as they are spherical when in suspension. Perfect packing for spherical objects results in 74% of a given volume being occupied. Equation 12 suggests that this reduces the number of cells that would be required to create a monolayer on the membrane surface.

65

That number is 391,825 cells. This number was rounded to an even 400,000 for future work.

$$\frac{Area_{membrane}}{Area_{circle}} = \frac{41.83 \; x \; 10^6 \mu m^2}{79 \mu m^2} \; x \; 1.0 = 529,494 \; cells \; (pf = 1.0) \qquad \text{(Equation 11)}$$

$$\frac{Area_{membrane}}{Area_{circle}} = \frac{41.83 \; x \; 10^6 \mu m^2}{79 \; \mu m^2} \; x \; 0.74 = 391,825 \; cells \; (pf = 0.74) \;) \qquad \text{(Equation 12)}$$

As previously explained, fusion protocols up to this point in the study introduced 400,000 cells in 50 µl into the chamber for fusion. This was equivalent to one monolayer of cells on the membrane. Since the addition of centrifugation resulted in well deposited cells, several tests were conducted to determine if larger numbers of cells could be deposited onto the membrane. This would create more than one layer of cells. This would not only increase the capacity of the chamber, but it could also increase cell to cell contact. Increases in cell to cell contact are desirable as they would most likely increase fusion yields. Basic tests revealed that 800,000 cells and 1.2 million cells could be deposited by centrifugation onto the membranes. Therefore the remaining work in this section introduced 1.2 million cells into the chambers to determine if improvements would result.

4.5.1 Fusion with Centrifugation and 1.2 million B16 Cells Deposited

B16 cells were stained with CMFDA and CMTMR for flow cytometric analysis. In one particular experiment, nine samples were analyzed in a similar manner as previous

66

cell fusion experiments. Samples, in sets of three were pulsed with an electrical field strength of 1500, 2000, and 2500 V/cm, respectively, a 300 μs pulse length, 8 pulses and a 1 second pulsing interval. The statistical mean total fusion yielded 16.4% ± 5.6 SD. The mean viable fusion was 3.2% ± 1.5 SD.

4.5.2 Fusion in Different Electroporation Buffers

After determining how well the fusion chamber performed with centrifugation and 1.2 million B16 cells deposited onto the membrane, the use of solutions other than PBS was investigated. Four solutions were used. The first was Electroporation Buffer (BTX). This was a commercially available solution. The second was Isoosmolar Buffer (Eppendorf). It was also a commercial product. These first two solutions were advertised to facilitate fusion and to decrease thermal effects on the cells which would increase viability, respectively. The third and fourth buffers were provided by Mr. Jose Rey, doctoral candidate. The composition of the third was 8.5% sucrose (w/v) and 0.3% glucose. The fourth was a diluted version of the third buffer containing a 1 to 5 ratio of 8.5% sucrose (w/v) and 0.3% glucose to sterile Millipore water. Both solutions were prepared in the Drug & Gene Delivery Lab. The motivation for investigating these solutions was a study using electroporation with Chinese Hamster Ovary (CHO) and B16-F1 cells. In this study, a hypotonic buffer was used to increase fusion yields (Ušaj, Trontelj et al. 2010).

Experiments were performed using CMFDA and CMTMR stained B16 cells were prepared as described above except that the cells were suspended in the appropriate buffer solution immediately prior to fusion. Identical experiments were performed for

67

each of the five buffers. Fusion was conducted in triplicate using electric fields of 1500, 2000, and 2500 V/m, respectively, a 300 μs pulse length, 8 pulses and a 1 second pulsing interval. Total and viable fusions were graphed to analyze the statistical differences the buffers may have in comparison to the standard DPBS that was regularly used for experimental analysis. These graphs show a consistency in higher fusion yields both in viable and total fusion.
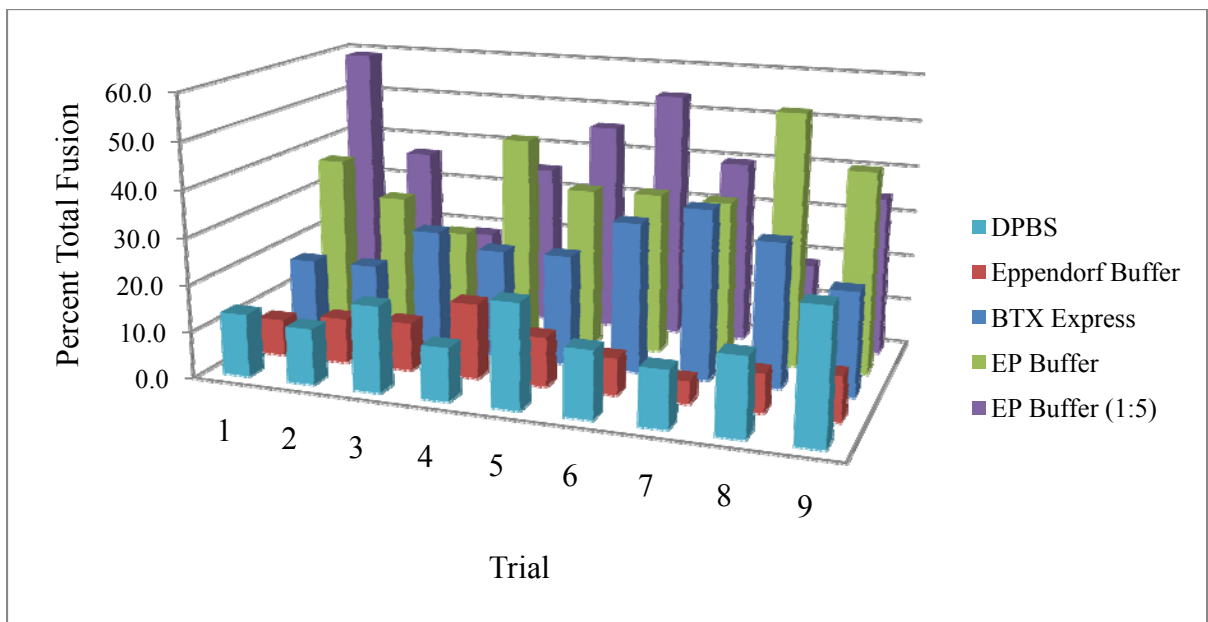
Figure 36. B16 to B16 Total Fusion vs. Electroporation Buffer.
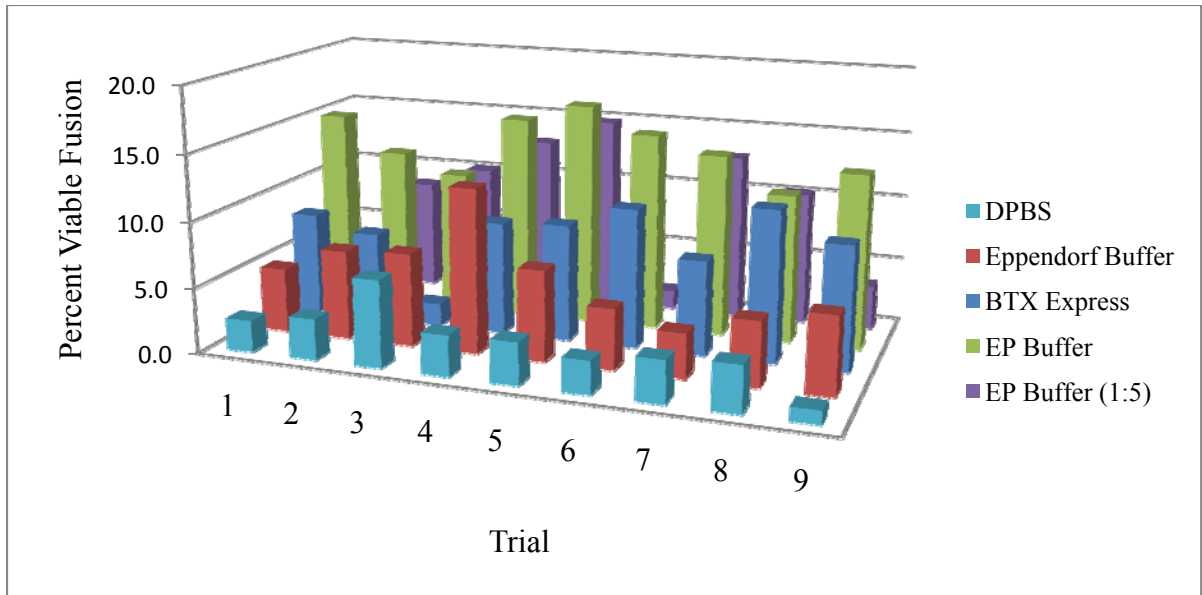
Figure 37. B16 to B16 Viable Fusion vs. Electroporation Buffer

Statistical data for the buffer solutions were calculated and are listed in Table 3. Mean
total and viable fusion yields were consistently higher in the lab synthesized
electroporation buffers. The first buffer, which contained 8.5% sucrose (w/v) and 0.3%
glucose, resulted total and viable fusion yields of 37.1% ± 9.3 SD and 13.8% ± 2.1 SD,
respectively. Additionally, the second buffer which contained a 1 to 5 ratio of 8.5%
sucrose (w/v) and 0.3% glucose to sterile Millipore water, resulted total and viable fusion
yields of 37.8% ± 13.9 SD and 8.3% ± 5.3 SD, respectively. These results showed
promise but additional research should be accomplished to validate reproducibility.

Table 3 Statistical Results for Electroporation Buffers

Solution	Field Strength (V/cm)	Total Fusion % ± SD (%Viable)	Viable Fusion % ± SD (%Viable)
DPBS	1500	14.5 ± 3.3	4.0 ± 2.3
DPBS	2000	15.9 ± 5.6	2.9 ± 0.4
DPBS	2500	18.9 ± 8.1	2.6 ± 1.4
BTX Express	2000	20.2 ± 5.3	5.5 ± 3.3
BTX Express	2000	26.4 ± 4.9	9.4 ± 1.1
BTX Express	2000	29.7 ± 7.2	9.4 ± 2.2
Eppendorf Buffer	2500	9.2 ± 1.3	6.3 ± 1.2
Eppendorf Buffer	2500	11.4 ± 4.2	8.0 ± 4.1
Eppendorf Buffer	2500	7.5 ± 2.4	4.7 ± 1.3
EP Buffer	1500	29.5 ± 7.2	12.6 ± 2.1
EP Buffer	1500	38.0 ± 5.7	15.9 ± 1.0
EP Buffer	1500	44.0 ± 10.1	12.8 ± 1.4
EP Buffer (1:5)	2000	38.1 ± 20.2	6.3 ± 5.2
EP Buffer (1:5)	2000	44.8 ± 9.3	9.7 ± 7.2
EP Buffer (1:5)	2000	30.7 ± 11.1	8.8 ± 4.8

Chapter 5. Discussion and Conclusions

5.1 Conclusions

Electrofusion is a process that can be used to fuse homogeneous and heterogeneous cell types by a phenomenon known as electropermeabilization. This temporary permeabilization renders cells fusogenic and can facilitate permanent cytometric fusion. Dielectrophoresis, which uses alternating current to align cells prior to electroporation, was not used in this research study because of the extreme heating and detriment to cellular activity. Cells were brought into contact using a novel electrofusion device in which an aliquot of a cell suspension at a desired concentration is placed on to a porous membrane. The solution from the suspension then passes through the porous membrane onto an absorbent pad leaving behind a thick cellular paste in which cells are in contact with each other. This cell to cell contact is necessary and promotes fusion of hybrids when cells are in a fusogenic state. One of the goals of this research was to investigate the fusogenic properties of various tissues and cell lines. B16 murine melanoma, human keratinocytes and neuroglioma cells were used in the initial stages of this research. Human sertoli cells were later provided by the Cell & Pathology Lab and were analyzed for their fusogenic characteristics. Cells were analyzed initially using fluorescent microscopy and once optimized, characterized by flow cytometry. Sertoli cells provide localized immunoprotection of cells or tissue grafts which can alleviate the need for systemic immunosuppressive medications. The device presented a novel

71

approach to electrofusion and has established a basis for future experiments. Homogeneous cell types that were fused, such as the B16, were reseeded post electroporation and were observed to readily proliferate. Additionally, the heterogeneous mix of B16 and HSC cells proliferated post electrofusion.

The 3rd generation electrofusion chamber worked well with several cell lines based on microscopy and flow cytometry and a protocol was implemented based on development, detection and quantitation of hybrid cells. The woven cellulose absorbent pad and microporous membrane were also characterized for their use in conjunction with the device. During fusion, the B16-F10 cell line resulted in 14.5% ± 3.3 SD at a 2000 V/cm electric field in preliminary studies. Additionally, fusion was increased to 18.9% ± 8.1 SD with an increased electric field of 2500 V/cm. Negative control samples were also collected and demonstrated an average 1.1% ± 0.8 SD of no fusion and should subtracted from total fusion results for increased accuracy. Prior to final fusion, it was noticed that assembly of the fusion device was critical. Significant leaking of cell suspensions occurred due to an insufficient seal between the device's electrodes, top and body. This problem was alleviated by depositing an excessive amount of epoxy during the build process and curing the epoxy for a minimum of twenty four hours. Leaking also occurred post fusion during the incubation stage. Incubation was critical after fusion because it allowed the fused hybrid cell membranes to anneal. The leaking may have occurred due to the breakdown of the epoxy during the pulsing process. To alleviate this dilemma, cells were removed from the electrofusion device immediately and placed in a 96 well plate for incubation. This type of mechanical manipulation may have lowered fusion results by maneuvering cells prior to the completion of the annealing process. To

72

alleviate the problem of leaking both pre and post electrofusion, the device should be built with an ultrasonic welder which would ensure a proper seal.

Cell clumping presented problems with quantitation as noticed with the characterization of the HaCaT and H4 cell lines. Dual fluorescence was illustrated in homogenous mixtures and would indicate fused hybrids of green and red stained cells. However, cell clumping presented obstacles in deciphering actual fusion. Ethylenediaminetetraacetic acid (EDTA) is a polyamino carboxylic acid that can be used in laboratory application such as cell culturing to bind to calcium and prevent the joining of cadherins between cells. Another alternative is to use Ethylenediamine-*N*,*N'*-disuccinic acid (EDDS) which can be used for the same process but is biodegradable and less toxic.

Centrifugation in conjunction with absorption enhances cell to cell contact and subsequently increases the production of fused hybrids. An initial fusion experiment that analyzed twenty samples of B16-F10 stained and fused cells resulted in an overall fusion yield of 7.7% ±3.4 SD. The first ten samples were applied a 2000 V/cm field strength, 300 μs pulse length with 8 pulses and yielded 7.8% ±3.9 SD fused hybrids. The second ten samples were applied a 2250 V/cm field strength, 300 μs pulse length with 8 pulses and yielded 7.7% ±3.2 SD fused hybrids. After centrifugation was incorporated into the protocol, comparable samples exposed to a 2000 and 2250 V/cm field strength, yielded 14.5% ± 3.3 SD and 15.9% ± 5.6 SD of fused hybrids, respectively. In addition to centrifugation, lab synthesized electroporation buffers also appeared to increase total and viable fusion. The composition of the first buffer contained 8.5% sucrose (w/v) and 0.3% glucose. Total and viable fusion yields were

73

increased to 37.1% ± 9.3 SD and 13.8% ± 2.1 SD, respectively. Additionally, the second buffer contained a 1 to 5 ratio of 8.5% sucrose (w/v) and 0.3% glucose to sterile Millipore water. This buffer also revealed increased total and viable fusion yields of 37.8% ± 13.9 SD and 8.3% ± 5.3 SD, respectively. The yields of the electroporation buffers need to be further analyzed to validate the fusion yields for reproducibility prior to confirmed incorporation in to the final protocol.

5.2 Recommendations for Future Research

Additional cell lines need to be investigated to further validate the usefulness of the novel electrofusion device. Cell lines with cadherins exhibiting adhesive effects that cannot be overcome with mild enzymes should be treated with chelating agents such EDTA or EDDS. This will facilitate a single cell suspension and ensure the accuracy of quantitation. B16 cells were consistent used in the trials of this research because of the ability to separate the cells in suspension. This was idea was discussed with one of the investigators on this project and may be used in future trials. The ultimate goal should be to bioengineer xenogenic and allogeneic cell hybrids for cell transplantation. The use of xenogenic tissues (tissue from other animals) has been successfully used in experimental animal models of diabetes, however immunosuppression is still required.

Fusion was accomplished several times in this research and was optimized by conducting several experiments and noting the electrical parameters. Absorption, using a microporous membrane and an absorbent pad, is a novel idea for cell to cell contact. However, this means did not increase cell to cell contact and promote fusion. It simply reduces the volume of the diluent temporarily before the cells adhere to the porous membrane and obstruct the pores. The incorporation of centrifugation proved to be a

74

noteworthy addition to this research study. Initial studies optimized centrifugation with the electrofusion cuvette using 100 RCF at 30°C for 1 minute. As studies continued and the build of the prototype created a better seal, the diluent still would not pass through the porous membrane. Again, this was due to 12 µm in diameter cells obstructing the passage of the diluent. This is vital because the electric field that is applied to the cell suspension may contact only affect the diluent and not the cells. This would negate the ability of rendering the cells fusogenic. In later studies, this was overcome by withdrawing approximately 20 µl of fluid from the top of the cuvette prior to electroporation. This may have also removed some cells due to the gentle centrifugation and lowered the desired cell concentration. To avoid this problem in future studies, the build of the cuvette should be considered. If a simple conical shape is added to the area where the cells are deposited, centrifugation could be used in conjunction with an electroporation facilitating substance. The shape would ensure no cell loss and may increase cell to cell contact and fusion yields. The diluent could then be aspirated, leaving a truly compacted cell pellet. The electrodes would need to extend into the cell pellet to deliver the energy accordingly. Lastly, the use of another material besides aluminum to increase cell and tissue viability could be employed. These changes could increase fusion yields and promote even more uses for electrofusion.

Prior to flow cytometry analysis, samples were suspended in DPBS for at least an hour prior to flow cytometry evaluation. DPBS is ideal for maintaining the pH of a sample for at least an hour or two but perhaps a medium rich in nutrients without phenol 5 red dye should be used to enhance viability.

75

The novel electrofusion device used in this research should be compared to devices that are currently on the market. There are several companies that have devices that use electroporation in suspension. This is in contrast to the design and use of our cuvette. Cell suspension samples should be electroporated and analyzed by fluorescent microscopy and flow cytometry to establish a baseline and device comparisons. However, these devices require AC and DC and it could be argued that this would not be an identical comparison. The Gene & Drug Delivery Lab has a Zimmerman Cell Fusion Power Supply that can be connected to the electrofusion cuvette holder to accomplish this study. The long term goal of this comparison would be to characterize fusion and viability.

References

Abidor, I. and Sowers, A. (1992). Kinetics and Mechanism of Cell Membrane Electrofusion. Biophysical Journal 1(61) 1557-1569.

Beebe, S. J., P. F. Blackmore, et al. (2004). Nanosecond Pulsed Electric Fields Modulate Cell Function Through Intracellular Signal Transduction Mechanisms. Physiological Measurement 25(4): 1077-1093.

Bhonde, R., Shukla, R.C., Kanitkar, M., Shukla, R., Banerjee, M. and Datar, S. (2007). Isolated Islets in Diabetes Research. Indian Journal of Medical Research, 125(3), 425.

Cameron, D. F., Hushen, J. J., Nazian, S. J., Willing, A., Saporta, S. and Sandberg, P. R. (2001), Formation of Sertoli Cell-Enriched Tissue Constructs Utilizing Simulated Microgravity Technology. Annals of the New York Academy of Sciences, 944: 420–428.

Cemazar, M., I. Wilson, Dachs, G., Tozer, G. and Serga, G. (2004). Direct Visualization of Electroporation-Assisted in vivo Gene Delivery to Tumors Using Intravital Microscopy – Spatial and Time Dependent Distribution. BMC Cancer Research Article 4(1): 81.

Chen, N., K. H. Schoenbach, et al. (2004). Leukemic Cell Intracellular Responses to Nanosecond Electric Fields. Biochemical and Biophysical Research Communications 317(2): 421-427.

Chui, K., A. Trivedi, et al. (2010). Characterization and Functionality of Proliferative Human Sertoli Cells. Cell Transplantation.

Connolly, R J., Lopez, G., Hoff, A. and Jaroszeski, M. (2009). Plasma Facilitated Delivery of DNA to Skin. Biotechnology and Bioengineering, 104(5), 1034.

Davalos, R. (2003). Theoretical Analysis of the Thermal Effects During in vivo Tissue Electroporation. Bioelectrochemistry 61(1-2): 99-107.

Davidson, R, Gerald P. (1975). Improved Techniques for the Induction of Mammalian Cell Hybridization by Polyethylene Glycol. Somatic Cell Genetics, 2(2), 165.

Davidson, R, O'Malley, K, Wheeler T. (1976). Polyethylene Glycol-Induced Mammalian Cell Hybridization: Effect of Polyethylene Glycol Molecular Weight and Concentration. Somatic Cell Genetics 2(3), 271.

77

Debruin, K. and Krassowska, W. (1999). Modeling Electroporation in a Single Cell I. Effects of Fields Strength and Rest Potential. Biophysical Journal 1(77) 1213-1224.

Degroot, M. (2004). Causes of Limited Survival of Microencapsulated Pancreatic Islet Grafts. Journal of Surgical Research 121(1): 141-150.

Feinstein, G., Hofstein, R., Koifmann, J. and Sokolovsky, M. (1974). Human Pancreatic Proteolytic Enzymes and Protein Inhibitors. European Journal of Biochemistry, 43(3), 569.

Frewin, C.L., Jaroszeski, M., Weeber, E., Muffly, K.E., Kumar, A., Peters, M., Oliveros, A., and Saddow, S.E. (2009). Atomic Force Microscopy Analysis of Central Nervous System Cell Morphology on Silicon Carbide and Diamond Substrates. Journal of Molecular Recognition, 22(5), 380.

Gabrijel, M. (2004). Quantification of Cell Hybridoma Yields with Confocal Microscopy and Flow Cytometry. Biochemical and Biophysical Research Communications 314(3): 717-723.

Gehl, J. (2003). Electroporation: Theory and Methods, Perspectives for Drug Delivery, Gene Therapy and Research. Acta Physiological Scandinavian Journal, 1(177) 437-447.

Golberg, A. and B. Rubinsky (2010). A Statistical Model for Multidimensional Irreversible Electroporation Cell Death in Tissue. BioMedical Engineering OnLine 9(1): 13.

Golzio, M. (2002). Direct Visualization at the Single-Cell Level of Electrically Mediated Gene Delivery. Proceedings of the National Academy of Sciences 99(3): 1292-1297.

Groot, M., Schuurs, T. and Schilfgaarde, R. (2004). Causes of Limited Survival of Microencapsulated Pancreatic Islet Grafts. Journal of Surgical Research. (121): 141-150.

Hayashi, T. (2002). Immunogenicity and Therapeutic Efficacy of Dendritic–Tumor Hybrid Cells Generated by Electrofusion. Clinical Immunology 104(1): 14-20.

Isaac, J., S. Skinner, et al. (2005). Transplantation of Neonatal Porcine Islets and Sertoli Cells Into Nonimmunosuppressed Nonhuman Primates. Transplantation Proceedings 37(1): 487-488.

Jaroszeski, M., Gilbert, R. and Heller, R. (1994). Detection and Quantitation of Cell-Cell Electrofusion Products by Flow Cytometry. Analytical Biochemistry, 216(2), 271.

Jaroszeski, M., Gilbert, R., Fallon, P. and Heller, R. (1994). Mechanically Facilitated Cell-Cell Electrofusion. Biophysical Journal, 67(4), 1574.

Jaroszeski, M., Heller, R. (1998). Flow Cytometry Protocols. New Jersey, Humana Press.

Jaroszeski, M., Heller, R., Gilbert, R. (2000). Electrochemotherapy, Electrogenetherapy, and Transdermal Drug Delivery; Electrically Mediated Delivery of Molecules to Cells. New Jersey, Humana Press.

Kim, J A., Cho, K., Shin, M.S., Lee, W.G., Jung, N., Chung, C. and Chang, J.K. (2008). A Novel Electroporation Method Using a Capillary and Wire-Type Electrode. Biosensors & Bioelectronics, 23(9), 1353.

Lehmann, B. (1997). HaCat Cell Line as a Model System for Vitamin D3 Metabolism in Human Skin. The Journal of Investigative Dermatology, 108(1), 78.

Lehninger, A. L., D. L. Nelson, et al. (2008). Lehninger Principles of Biochemistry. New York, W.H. Freeman.

Lindner, M. (2002). Tumour Cell–Dendritic Cell Fusion for Cancer Immunotherapy: Comparison of Therapeutic Efficiency of Polyethylene-Glycol versus Electro-Fusion Protocols. European Journal of Clinical Investigation, 32(3), 207.

Li, F., X. Zhou, Zhu, J., Ma, J., Huang, X. and Wong S. (2007). High Content Image Analysis for Human H4 Neuroglioma Cells Exposed to CuO Nanoparticles. BMC Biotechnology 7(1): 66.

Lin, H. P., C. Vincenz, Eliceiri, K., Kerppola, T. and Ogle, B. (2010). Bimolecular Fluorescence Complementation Analysis of Eukaryotic Fusion Products. Biology of the Cell. 102(9): 525-537.

McClenaghan, N H. (1996). Characterization of a Novel Glucose-Responsive Insulin-Secreting Cell Line, BRIN-BD11, Produced by Electrofusion. Diabetes, 45(8), 1132.

Mekid, H. (2000). In vivo cell electrofusion. Biochimica et Biophysica Acta. G, General subjects, 1524(2-3), 118.

Meldrum, R., Bowl, M., Ong, S.B. and Richardson, S. (1999) Optimisation of Electroporation for Biochemical Experiments in Live Cells. Biochemical and Biophysical Research Communications 256(1) 235-239.

Needham, D. and Hochmuth, R.M. (1989). Electro-Mechanical Permeabilization of Lipid Vesicles: Role of Membrane Tension and Compressibility. Biophysical Journal 1(55) 1001-1009.

Neumann, E., Schaffer-Ridder, M., Wang, Y., and Hofschneider, P.H. (1982). Gene Transfer Into Mouse Lyoma Cells by Electroporation in High Electric Fields. The EMBO Journal, 1(7): 841.

Neumann, E., Sowers, A., Jordan, C. (1989). Electroporation and Electrofusion in Cell Biology. New York, Plenum Press.

Nikolsky, V. and Efimov, I. (2005). Electroporation of the Heart. The European Society of Cardiology, 7(2), S146.

Panday, Shivanand. (2010). Hybridoma Technology for Production of Monoclonal Antibodies. International Journal of Pharmaceutical Sciences Review and Research, 1(2), 88.

Pileggi, A, Ricordi, C, Kenyon, N S, et al. (2004). Twenty Years of Clinical Islet Transplantation at the Diabetes Research Institute-University of Miami. Clinical Transplants,177-204.

Ramos, A., Suzuki, D. and Marques, J. (2004). Numerical Simulation of Electroporation in Spherical Cells. Artificial Organs, 28(4), 357.

Rols, M P., Teissié, J. (1990). Electropermeabilization of Mammalian Cells. Quantitative Analysis of the Phenomenon. Biophysical Journal, 58(5), 1089.

Rols, M P. and Teissié, J. (1998). Electropermeabilization of Mammalian Cells to Macromolecules: Control by Pulse Duration. Biophysical Journal, 75(3), 1415.

Rols, M. P., F. Dahhou, et al. (1994). Pulse-First Heterofusion of Cells by Electric-Field Pulses and Associated Loading of Macromolecules into Mammalian-Cells. Biotechniques 17(4): 762-&.

Rudnick, A., Ling, T.Y., Odagiri, H., Rutter, W.J. and German, M.S. (1994). Pancreatic Beta Cells Express a Diverse Set of Homeobox Genes. Biochemistry, 1(19), 12203

Sanberg, P R. (1996). Testis-Derived Sertoli Cells Survive and Provide Localized Immunoprotection for Xenografts in Rat Brain. Nature Biotechnology, 14(13), 1692.

Sanberg, P R. (1997). Testis-Derived Sertoli Cells Have a Trophic Effect on Dopamine Neurons and Alleviate Hemiparkinsonism in Rats. Nature Medicine, 3(10), 1129.

Shivanand, P. (2010). Hybridoma Technology for Production of Monoclonal Antibodies. International Journal of Pharmaceutical Sciences Review and Research, 1(2), 88.

Skelley, A M. (2009). Microfluidic Control of Cell Pairing and Fusion. Nature Methods, 6(2), 147.

Stenger, D., Kaler, K. and Hui S.W. (1991). Dipole Interactions in Electrofusion; Contributions of Membrane Potential and Effective Dipole Interaction Pressures. Biophysical Journal, (59) 1074-1084.

Tarek, M. (2005). Membrane Electroporation: A Molecular Dynamics Simulation. Biophysical Journal, 88(6), 4045.

Teissie, J., M. Golzio, et al. (2005). Mechanisms of Cell Membrane Electropermeabilization: A Minireview of our Present Knowledge. Biochimica et Biophysica Acta (BBA) - General Subjects 1724(3): 270-280.

Terada, N. (2002). Bone Marrow Cells Adopt the Phenotype of Other Cells by Spontaneous Cell Fusion. Nature, 416(6880), 542.

Tieleman, D P. (2004). The Molecular Basis of Electroporation. BMC Biochemistry, 5(1): 10.

Tsong, T. (1991). Electroporation of Cell Membranes. Biophysical Journal, 1(60) 297.

Ušaj, M., K. Trontelj, Miklavčič, D. and Kandušer, M. (2010). Cell–Cell Electrofusion: Optimization of Electric Field Amplitude and Hypotonic Treatment for Mouse Melanoma (B16-F1) and Chinese Hamster Ovary (CHO) Cells. The Journal of Membrane Biology 236(1): 107-116.

Valdes-Gonzalez, R. A. (2005). Xenotransplantation of Porcine Neonatal Islets of Langerhans and Sertoli cells: A 4-Year Study. European Journal of Endocrinology 153(3): 419-427.

von Keller, A., Tewinkel, M., Wingender, R., Volkmann, D. and Schnabl H. (1995). Intracellular Movements and Reorganization of Electrically Fused Sunflower Protoplasts. International Journal of Plant Sciences, 156(6), 764.

Wade, L. G. (2006). Organic chemistry. Upper Saddle River, N.J., Pearson Prentice Hall.

Walker, M. D. (2008). Role of MicroRNA in Pancreatic Cells: Where More Is Less. Diabetes 57(10): 2567-2568.

Wang, D Z., Skinner, S., Escobar, L., Salto-Tellez, M., Garkavenko, O., Khoo, A., Lee, K.O., Calne, R. and Isaac, J.R. (2005). Xenotransplantation of Neonatal Porcine Islets and Sertoli Sells Into Nonimmunosuppressed Streptozotocin-Induced Diabetic Rats. Transplantation Proceedings, 37(1), 470.

Weaver, J C. and Chizmadzhev, Y.A. (1996). Theory of Electroporation: A Review. Bioelectrochemistry and Bioenergetics, 41(2), 135.

Willing, A E. (1998). Sertoli Cell Transplants: Their Use in the Treatment of Neurodegenerative Disease. Molecular Medicine Today, 4(11), 471.

Yang, Y.-G. and M. Sykes (2007). Xenotransplantation: Current Status and a Perspective on the Future. Nature Reviews Immunology 07(07): 519-531.

Zimmermann, U. (2002). Electromanipulation of Mammalian Cells: Fundamentals and Application. IEEE Transactions on Plasma Science, 28(1),72.

81

Zimmermann, U. and Pilwat, G. (1982). Electric Field-Mediated Cell Fusion. Journal of Biological Physics 10(1): 43-50.

Zimmermann, U., Pilwat, G. and Riemann, F. (1974). Dielectric Breakdown of Cell Membranes. Biophysical Journal 1(14): 881-899.

Zimmermann, U., Friedrich U., Mussauer, H., Gessner, P., Hämel, K., Sukhorukov, V. (2002). Electromanipulation of Mammalian Cells: Fundamentals and Application. IEEE Transactions on Plasma Science, 28(1),72.

Zimmermann, W.-H., Melnychenko, I., Wasmeier, G., Didi, M., Naito, H., Nixdorff, U., Hess, A., Budinsky, L., Brune, K., Michaelis, B., Dhein, S., Schwoerer, A., Ehmke, H. and Eschenhagen, T. (2006). Engineered Heart Tissue Grafts Improve Systolic and Diastolic Function in Infarcted Rat Hearts." Nature Medicine 12(4): 452-458.

About the Author

The author began studying chemical engineering at North Carolina State University. He later pursued a clinical career in the United States Air Force as an emergency medical technician (EMT) gaining invaluable medical device and patient care experience. While continuing to work as an EMT, the author continued his pursuit towards an engineering education. The clinical aspect of the military allowed the author to understand that a mesh of methodical, problem solving, engineering skills and hands on clinical training could be of great benefit to the engineering and healthcare industries. The author later transitioned from a full time military member to a full time student in order to complete his chemical engineering bachelor's degree and later his biomedical engineering master's degree. The author completed research in both the bioengineering and tissue engineering subdisciplines and later worked part time as an intern for an electrosurgical device company prior to transitioning back to the medical industry.